Universiteit
Leiden
The Netherlands

Starlight beneath the waves : in search of TeV photon emission from Gamma-Ray Bursts with the ANTARES Neutrino Telescope

Laksmana-Astraatmadja, T.

Citation
Laksmana-Astraatmadja, T. (2013, March 26). *Starlight beneath the waves : in search of TeV photon emission from Gamma-Ray Bursts with the ANTARES Neutrino Telescope*. *Casimir PhD Series*. Retrieved from https://hdl.handle.net/1887/20680

Version:	Not Applicable (or Unknown)
License:	Leiden University Non-exclusive license
Downloaded from:	https://hdl.handle.net/1887/20680

Note: To cite this publication please use the final published version (if applicable).

Cover Page

Universiteit Leiden

The handle http://hdl.handle.net/1887/20680 holds various files of this Leiden University dissertation.

Author: Astraatmadja, Tri Laksmana
Title: Starlight beneath the waves : in search of TeV photon emission from Gamma-Ray Bursts with the ANTARES Neutrino Telescope
Issue Date: 2013-03-26

1 Introduction

The idea on which this dissertation is based is a very old one, but today can become a reality with the recent advent of very large volume neutrino telescopes.

When a downgoing high-energy γ-ray passes through the atmosphere of the Earth, it will interact with the particles in the atmosphere and initiate an electromagnetic shower of particles (not unlike what is shown in Figure 1.1). This shower could produce, among others, a small number of muons that can penetrate deep into the Earth, losing their energy along the way. If a muon moves with a speed exceeding the speed of light in its surrounding medium, the medium will radiate so-called Čerenkov photons at a characteristic angle relative to the direction of the muon. An undersea or under-ice large-volume neutrino telescope can detect the surviving muons by detecting these Čerenkov photons. The Čerenkov photons are recorded by the light-sensitive photomultiplier tubes that comprise the neutrino telescope. By finding signals causally connected in space and time, the track of a muon can be reconstructed to obtain the energy of the muon and its direction of arrival. A neutrino telescope primarily intended to observe upgoing neutrino-induced muons could then have a secondary function as a γ-ray telescope.

With the completed construction of the ANTARES[1] neutrino telescope in the Mediterranean Sea (Ageron et al., 2011) and IceCube[2] at the South Pole (Halzen & Klein, 2010), it is now possible to revisit this old idea of using a neutrino detector as a γ-ray telescope. The goal of this dissertation is to find out whether this is actually possible, to study the response of the detector to downgoing muons if that is the case, and also to perform an analysis of the now-available data from ANTARES.

This method of γ-ray detection can in principle be applied to any astrophysical source that emits high-energy γ-rays. However for reasons that will be discussed later on, in this dissertation gamma-ray bursts (GRB) will be the sole target of the attempt to detect high-energy γ-rays using an underwater large-volume neutrino telescope.

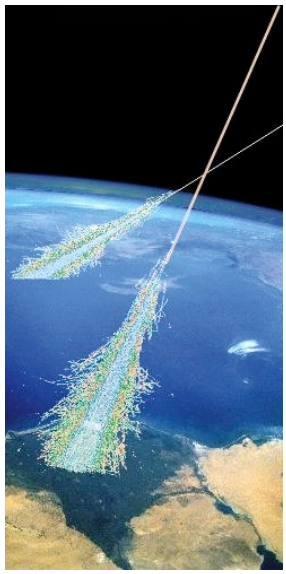

Figure 1.1: An illustration of a particle shower initiated by cosmic rays. Credit: Simon Swordy (University of Chicago, NASA).

[1] Astronomy with a Neutrino Telescope and Abyss environmental RESearch project, `http://antares.in2p3.fr`

[2] `http://icecube.wisc.edu/`

Many things need to be outlined first before we venture deeper into this endeavour. In the following subsections I will outline the leitmotif that drives this particular line of research and elaborate upon the basic idea described above.

1.1 Photon, cosmic ray, and neutrino astronomy

On all of its surface and at all times, the Earth is bathed with particles. They are emitted from various astronomical sources and produced by various physical processes. They carry information on the nature of the astronomical sources from which they are produced. In order to comprehend the workings of the universe, astronomers build various instruments to detect these particles and interpret the results.

Among these particles are the photons, carriers of the electromagnetic force. Starlight, i.e. photon emissions from astronomical sources, has inspired generations of natural philosophers since time immemorial. Gods were made, myths and religions were built, and musings concerning the nature of the sources were thought out (Krupp, 1994). It can be said that the traditional method of astronomical observation is carried out by observing photons emissions from celestial sources, hence in hindsight it can also be classified as *photon astronomy*.

Photon astronomy as a modern science began when Hans Lippershey, a Dutch-German lensmaker who lived in Middelburg, The Netherlands, developed the first known optical telescope in 1608 (van Helden, 1977). The development of photographic plates in the mid-19th century and their usage in astronomy as a mean to permanently record astronomical observations can only accelerate our progress in astronomical research (de Vaucouleurs, 1961), and the same could be said with the development of spectroscopy—pioneered by German optician Joseph Fraunhofer in 1814—as a method to decompose a beam of light into its constituent lights of different wavelengths. Nowadays the instruments of the photon astronomers are as varied as the energy regimes and sources of the photons. From radio waves to high-energy γ-rays, the electromagnetic spectrum has been thoroughly explored, and multiwave-

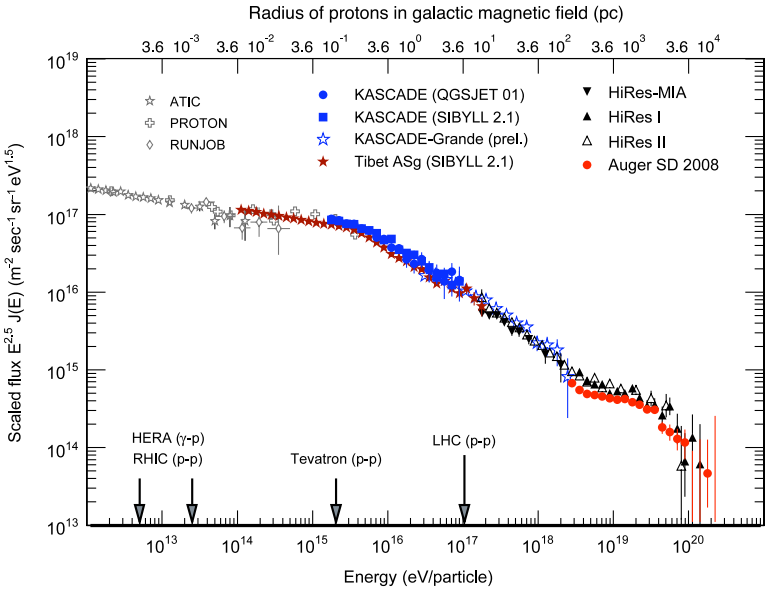

Figure 1.2: The energy spectrum of cosmic rays, reproduced from Hörandel (2010).

length astronomy has become the norm in photon astronomy.

Aside from photons, cosmic rays also constantly bombard the Earth. They are fully ionized atomic nuclei accelerated to relativistic velocities. Their interactions with the nuclei in the atmosphere produce showers of particles (Figure 1.1) that could be detected at the surface of the Earth. They were first discovered by Victor Hess through a series of balloon experiments (Figure 1.3) to measure the change of ionization level in the Earth's atmosphere. The prevailing view at that time was that the Earth is the source of ionizing radiation and thus the rate should decrease as we ascend to higher altitude. Hess however measured instead an increasing rate of ionization with increasing altitude, and concluded that the radiation that penetrates the atmosphere comes from outer space (Hess, 1912).

Figure 1.3: Victor Hess preparing for his balloon ascent to measure cosmic rays, Austria, 1912. Credit: American Physical Society (APS), http://www.aps.org

The energy spectrum of cosmic rays (Figure 1.2) stretch from below 100 Megaelectronvolt (MeV) up to 10^{20} eV. At very high energy, the energy gained from their acceleration exceeds anything that could be performed in the largest manmade particle acceler-

ators on Earth. How these natural accelerators could accelerate particles to such enormous level of energy is a mystery that still puzzle scientists up to this day.

Efforts to pinpoint their sources and thus obtain a better understanding of the acceleration mechanism are however hampered by the fact that cosmic rays are charged particles and could thus get deflected to random directions by ambient magnetic fields. Only cosmic rays of the highest energies are minimally deflected by magnetic fields and could thus point back relatively close to their sources, but these events are very rare (approximately one 10^{19} eV particle per km^2 per year per steradian) and their observation would require a detector with a very large collecting area so that enough particles could be detected within reasonable observation time. The Pierre Auger Observatory[3] (Abraham et al., 2004) is currently the largest cosmic ray observatory in the world, operating at Malargüe in Argentina.

[3] http://www.auger.org

It is now generally accepted that cosmic rays with energies below 100 MeV come from the Sun. Cosmic rays with energies up to 10^{15} eV (the so-called "knee" in the cosmic ray energy spectrum) are usually considered to be Galactic in nature. The most possible accelerators are the supernova remnants (SNRs). As the shock front of the supernova propagates through the interstellar medium, repeated scattering of the particles across the shock front enable them to gain energy (Blandford & Eichler, 1987).

Cosmic rays with energies above 10^{18} eV are considered to be accelerated at extragalactic sites such as active galactic nuclei (AGN) or gamma-ray bursts (GRB) (Hörandel, 2010). These two sources are an attractive candidate because their total energy output is roughly equal to the total energy output of observed extragalactic cosmic rays (Gaisser, 1997; Halzen, 2007). If we integrate the energy spectrum of extragalactic cosmic rays to obtain their energy density ρ_E, we will arrive at roughly $\rho_E = 10^{-19}$ TeV cm^{-3}. In order to generate an energy density with that magnitude over a period of 10^{10} years, a population of sources would have to release $\sim 3 \times 10^{37}$ erg s^{-2} Mpc^{-3}. This required energy release corresponds roughly to $\sim 2 \times 10^{44}$ erg per AGN or $\sim 2 \times 10^{52}$ erg per GRBs, which is coincident with the the observed output in electromagnetic energy of these sources.

To confirm that GRBs or AGN are the primary sources of cosmic rays is difficult because of the aforementioned reason that they are deflected by ambient magnetic fields. However, the interaction of cosmic rays with the ambient matters produce secondary particles that does not interact with magnetic fields and points back to its source: very-high energy (VHE) photons—which is of particular interest to this dissertation—and ultra-high energy (UHE) neutrinos. Thus the motivation to understand the origin of cosmic rays at the highest energy is linked with the motivation of this dissertation and is also inextricably related to the search of high-energy neutrinos. Next we shall discuss on how by searching for VHE photons and UHE neutrinos could aid in pinpointing the exact location of cosmic rays.

Neutrinos are another kind of particle that have interest astronomers soon after their discovery in 1956 (Cowan et al., 1956), since they are also produced in the nuclear fusion reaction that powers the Sun (Fowler, 1958). Because of the high density at the core of the Sun, photons took hundreds of thousands of years ricocheting through the Sun before they finally escape and reach Earth. On the other hand, neutrinos interact very weakly with matter and could travel unimpeded throughout the Sun. Neutrinos are then an important carrier of information about what is going on at the core of the Sun, deep under the photosphere and is hidden from the observations of photon astronomers. Their weak interaction with matters, on the other hand, makes their detection difficult. Neutrino astronomy was born when the first detection of solar neutrinos was made (Davis, Harmer & Hoffman, 1968).

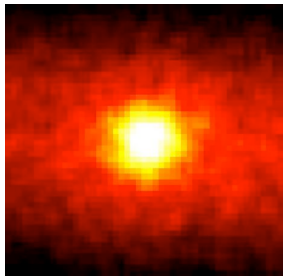

Figure 1.4: A Super-Kamiokande neutrino image of the Sun. The center of this image is the position of the Sun, and the size of the image is $90^\circ \times 90^\circ$. Brighter colors represent the higher flux of neutrinos. This image is made using 500 days of Super-K data. Credit: Robert Svoboda and K. Gordan, Louisiana State University. Retrieved from Astronomy Picture of the Day (APOD).

Up to the time of writing, the astrophysical neutrino sources thus far discovered are only the Sun and Supernova (SN) 1987A (Hirata et al., 1987; Bionta et al., 1987), which emits neutrinos with relatively low-energy, i.e. in the MeV regime. However, the neutrino energy spectrum (Figure 1.5) extends from the very low energies of 1.9 Kelvin cosmic neutrino background (CNB) radiation to the very high at the EeV regime. CNB might never be directly detected although it is possible to indirectly detect them by analysing the power spectrum of the CMB (De Bernardis et al., 2008). Aside from the Sun and SN 1987A, atmospheric neutri-

The cosmic neutrino background (CNB) is the neutrino counterpart to the cosmic microwave background (CMB). The CNB decoupling from matters occured when the universe was a mere 2 second old.

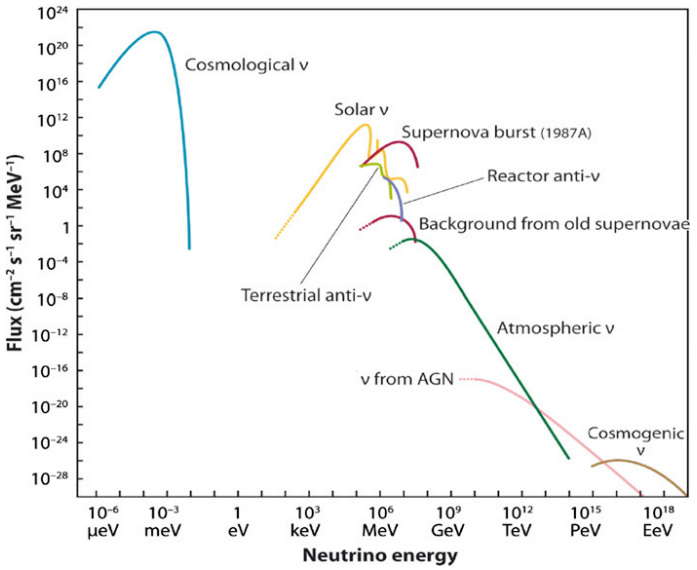

Figure 1.5: The energy spectrum of natural and reactor neutrinos, reproduced from Katz & Spiering (2012).

nos produced from cosmic-ray interactions with the Earth's atmosphere have also been regularly detected (Gaisser, 2011). Ultra high-energy (UHE) neutrinos from astrophysical sources are still awaiting detection and will probably be detected within the next decade by existing or future very large volume neutrino telescopes.

Observing UHE neutrinos is the tell-tale sign for the acceleration site of cosmic rays. The emission of high-energy neutrinos is expected as a consequence of the interaction between cosmic rays with ambient matter. A relativistically expanding matter will interact with its surrounding environment and create a shock wave. Shock-accelerated protons could escape and be observed on Earth as cosmic rays, but some will interact dominantly with photons to produce Delta resonances which will subsequently decay into charged pions (Waxman & Bahcall, 1997):

$$p\gamma \rightarrow \Delta^+ \rightarrow n\pi^+ \tag{1.1}$$
$$\pi^+ \rightarrow \nu_\mu + \mu^+ \tag{1.2}$$
$$\mu^+ \rightarrow \bar{\nu}_\mu + e^+ + \nu_e \tag{1.3}$$
$$n \rightarrow p + e^- \tag{1.4}$$

As we can see, the resulting neutrino flavour ratio at the source is approximately $\nu_e : \nu_\mu : \nu_\tau = 1 : 2 : 0$. If we assume that the secondary pions receive 20% of the proton energy for each interaction, and each secondary lepton shares $1/4$ of the pion energy, each flavor of neutrino is then emitted with 5% of the proton energy which is dominantly in the PeV regime (Mészáros, 2006).

As has mentioned before, GRBs are an attractive candidate as the source of cosmic-rays because their total energetics "suspiciously" match the integrated energy of cosmic rays. It is possible then that this injected energy is converted into the production of cosmic rays. Observing UHE neutrinos could establish the corresponding source—be it AGN or GRBs—as the source of extragalactic cosmic rays. Since most GRBs are located at cosmological distances with a redshift $z \sim 1$, detecting neutrinos from each individual GRBs might not be possible. However, nearby GRBs do occur and it may be possible for a km-scale neutrino telescope to detect neutrinos from these objects. In addition, the detection of UHE neutrinos is also important in understanding the internal mechanism of the probed source, e.g. GRBs: particle acceleration, radiation mechanism, and the progenitor itself could be characterized.

VERY-HIGH energy photons could also be produced from the interaction of cosmic rays with ambient matters. The first channel that can be considered is through the production of Delta resonance:

$$p\gamma \rightarrow \Delta^+ \rightarrow \pi^0 + p, \tag{1.5}$$

$$\pi^0 \rightarrow \gamma\gamma, \tag{1.6}$$

here π^0 will decay into VHE photons. Another way to produce VHE photons is through the Inverse Compton (IC) mechanism:

$$e^- + \gamma \rightarrow e^- + \gamma, \tag{1.7}$$

here low-energy photons γ are scattered by relativistic electrons and thus gain energy, becoming high-energy photons γ.

The first channel can be an important contribution to the total flux provided there are protons accelerated in significant number and that their energy exceeds that of the VHE photon by at least

one order of magnitude. The proton spectral index should be hard, e.g. $dN/d\epsilon_p \propto \epsilon_p^{-2}$ rather than $\epsilon_p^{-2.2}$, otherwise there will not be enough protons to produce VHE photons and the $p\gamma$ channel will be a less important channel than the IC component (Mészáros, 2006).

Another variation of the IC process is the synchrotron-self Compton (SSC) process in which the photons are provided by the synchrotron radiation from accelerated electrons. This model is leptonic in nature, i.e. pure electron acceleration model, and not hadronic. This means that they do not directly explain the origin of cosmic rays. In most realistic cases, however, both hadronic and leptonic models do take place. Observing VHE photons from GRBs could then provide not only hints on the origin of cosmic rays but also on the acceleration mechanisms of hadrons and leptons in the source. The production of VHE photons will be elaborated in Section 2.1.

The main problem that troubles observations of VHE photons is the fact that they interact very strongly with ambient infrared photons to produce pairs of electron-positron. The universe is transparent to photons up to $\epsilon_\gamma \sim 10$ GeV, but at $\epsilon_\gamma = 1$ TeV the mean free path is only a few hundred Mpc (Finke, Razzaque & Dermer, 2010). This limits our observational window only to nearby GRBs, which very rarely go off at such nearby distance. However, one can hope as such an event has happened in the past, e.g Galama et al. (1998); Mirabal et al. (2006); Starling et al. (2011).

1.2 *Gamma-ray burst astronomy*

GAMMA-RAY BURSTS are a brief flash of γ-rays occuring approximately once per day at random time and direction in space (Fishman & Meegan, 1995; van Paradijs, Kouveliotou & Wijers, 2000; Woosley & Bloom, 2006; Gehrels, Ramirez-Ruiz & Fox, 2009). In this brief moment, the γ-radiation lit up the otherwise dark γ-ray sky, outshining any other γ-ray sources. Their spatial directions are isotropically distributed and so far are found to be nonrepeating. The γ-ray production mechanism of GRBs are thought to involve particles accelerated to ultrarelativistic speeds and colli-

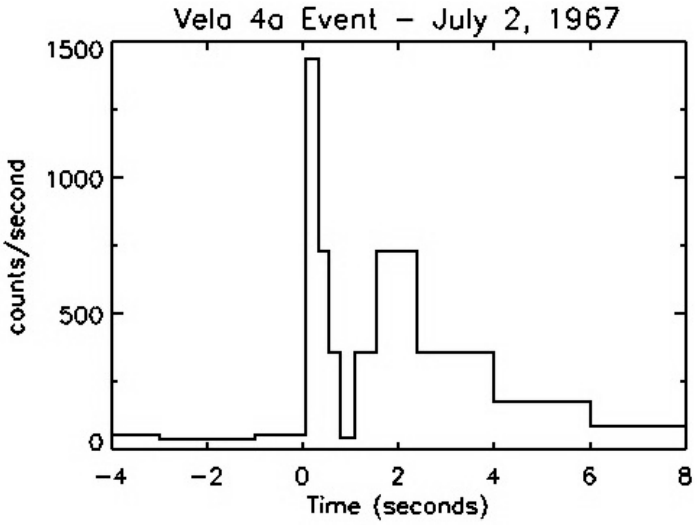

Figure 1.6: The first ever GRB signature detected by *Vela*. Credit: Goddard Space Flight Center.

mated into bipolar jets (e.g. Rees & Mészáros 1992, Mészáros & Rees 2001). The total energy output in γ-rays for a typical GRB, corrected for beaming effects, is $\sim 10^{51}$ erg (Woosley & Bloom, 2006).

The discovery of GRBs is a quintessential example of serendipity in scientific endeavour. In the midst of the Cold War and the looming threat of an all-out nuclear war, the Nuclear Test Ban Treaty was signed in July 1963 by the governments of the Soviet Union, United Kingdom, and the United States. The treaty prohibits nuclear detonation test anywhere except underground. To assure compliance to this treaty, the United States government launched a series of satellites called *Vela* (Figure 1.7) to detect any nuclear test conducted in space or in the atmosphere.

Figure 1.7: The *Vela* 5B satellite. Credit: NASA.

In 1967, *Vela* 4A detected a flash of γ-radiation which time profile showed a double-peaked curve (Figure 1.6): a short intense peak followed by a softer but prolonged peak. Although this is a tell-tale signature of a nuclear explosion, it was later clear that this gamma-ray burst did not come from a nuclear explosion. The intense first peak shown in Figure 1.6 is much too long for an atmospheric nuclear test, which duration lasts typically in the order of miliseconds. Several bursts of this nature were later detected,

but the military nature of the *Vela* mission kept this discovery from going public until 1973, when it was finally declassified and published by Klebesadel, Strong & Olson (1973). This was confirmed shortly after by Soviet scientists who observed similar bursts detected by the satellite Kosmos 461 (Mazets, Golenetskij & Il'Inskij, 1974).

Serendipity is characterized by a "happy accident", i.e. finding an unforeseeable event that turns out to be better than what could be foreseen by the original intent. What was meant to be a rather mundane task of detecting nuclear test in space—some sort of an anti-shoplifting mirror in space—turns out to be one of the greatest mysteries astronomers ever faced.

The anti-shoplifting-mirror-in-space analogy was described by Ralph Wijers in one of his lectures on GRB: "If you own a shop and you don't trust your customers, you put mirrors at the corners to prevent shoplifters. In the Cold War you put satellites in space to make sure the other side keep their side of the bargain."

THE DIRECTION of γ-rays is notoriously difficult to pinpoint. This difficulty hampered early attempts to understand GRBs. A first attempt to determine their direction was performed by triangulation using the arrival time of the γ-rays at different satellites. This way, the Interplanetary Network (IPN) of six satellites managed to localize GRBs with uncertainty up to within arcminutes from their actual location (Vedrenne, 1981; Cline et al., 1981). No optical counterpart, however, was found within this error circle. There was no way to determine the distance to the GRBs either, and thus without any knowledge of their intrinsic brightness it was next to impossible to discern the true nature of GRBs.

In the face of this gross lack of observational data, controversies and wild speculations were rampant. Since the discovery of GRBs up to 1995, about 2000 papers have been published about GRBs (Fishman & Meegan, 1995). Theories abound on their nature, ranging from the exotic which involves cosmic strings (e.g. Paczyński, 1988) to the rather standard such as comets impacting a neutron star (e.g. Tremaine & Żytkow, 1986), or even simple local events such as the scattering of solar photons by relativistic dust grains (e.g. Grindlay & Fazio, 1974). Ideas kept popping out and at one point there were about 100 competing models that tried to explain GRBs (Nemiroff, 1994). One of the main issues of this debate is whether GRBs are local events or located at cosmological distances.

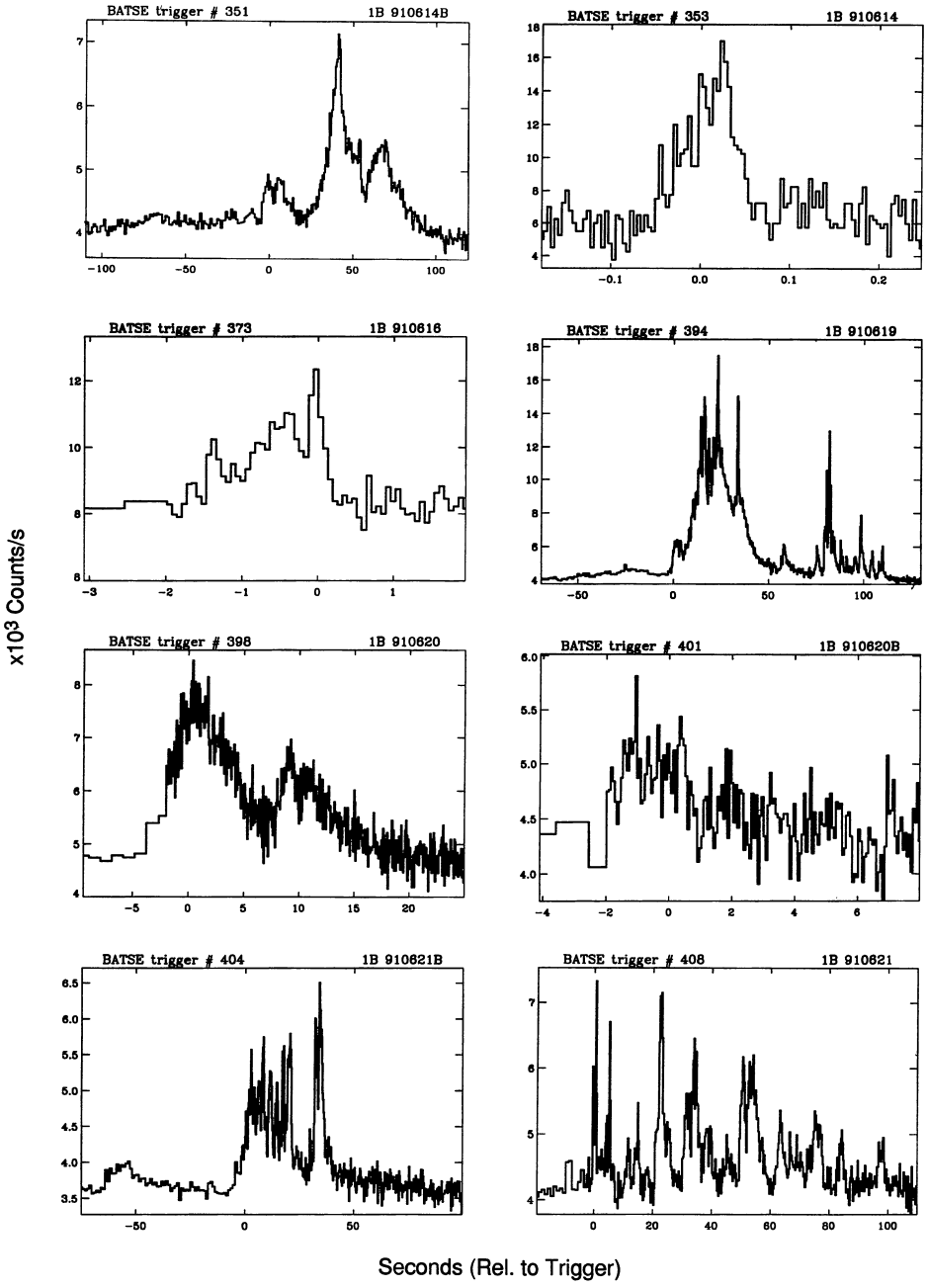

Figure 1.8: A sample of several GRB light curves from the First BATSE Gamma-Ray Burst Catalog (Fishman et al., 1994). The profile of the light curves exhibit a variety in their profiles, intensities, and duration.

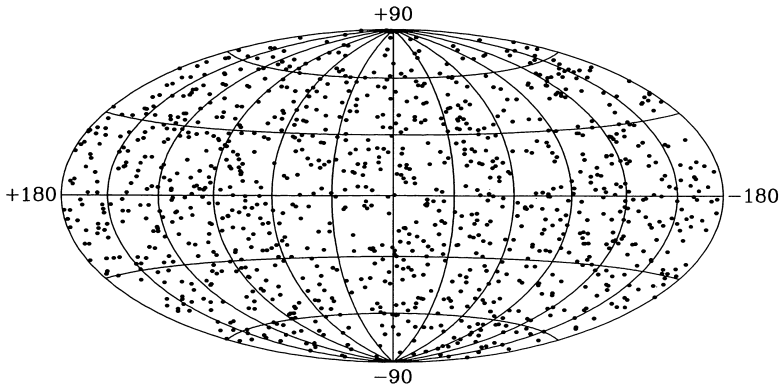

Figure 1.9: The sky distribution of the 1122 GRBs from the BATSE 3B catalog, mapped on Hammer-Aitoff projection in Galactic coordinates. The isotropic distribution of the GRB directions suggests that they are located at cosmological distances. The map is reproduced from Meegan et al. (1996).

Progress in our observational knowledge of GRBs before 1997 was mostly obtained from the observations of the γ-ray detector BATSE[4] on board the *Compton Gamma-Ray Observatory* (CGRO)[5]. In BATSE, NaI crystals are used as a scintillator which is sensitive to γ-rays with energies from $\sim$25 to 2000 keV (Paciesas et al., 1999). This wide energy range makes BATSE very sensitive and thus enable it to detect 2 or 3 GRBs on a typical day. To complement BATSE, *Compton* also carried with it the EGRET[6] instrument, a multilevel thin-plate spark chamber that produces pairs of electron-positron upon impact with a γ-ray (Kanbach et al., 1988). EGRET is sensitive to γ-rays from 20 MeV to 40 GeV and is thus suitable to probe the high-energy component of a GRB.

Between 1991 and 2000 BATSE observed 2704 GRBs. Their spatial distribution indicates an isotropic angular distribution (Figure 1.9) which implies that GRBs must be located at cosmological distances (Meegan et al., 1992; Briggs et al., 1996), or at least located at the halo of our Galaxy (Podsiadlowski, Rees & Ruderman, 1995). If GRBs are located at cosmological distances, consequently their energy output should be extremely huge. This narrows down the possible theoretical explanations.

Two other BATSE results of note will be described here. The first is the realization that the time-averaged energy spectrum of a GRB emission can be well-described at low energy by a power-law function with an exponential cutoff (Band et al., 1993, Figure

[4] Burst And Transient Source Experiment, `http://www.batse.msfc.nasa.gov/batse/`

[5] `http://heasarc.gsfc.nasa.gov/docs/cgro/`

[6] Energetic Gamma-Ray Experiment Telescope, `http://heasarc.gsfc.nasa.gov/docs/cgro/egret/`

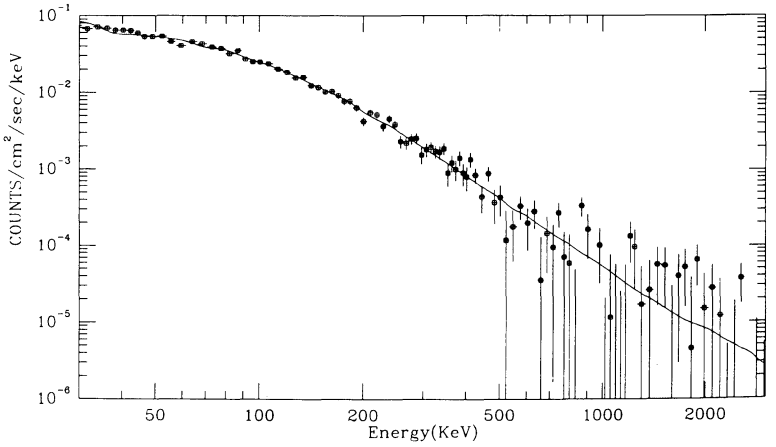

Figure 1.10: An example of a GRB photon spectral density and the spectral fitting of the Band function to the data, here reproduced from Band et al. (1993). The GRB shown here is GRB 1B 911127. The low-energy spectral index is $\alpha = -0.968 \pm 0.022$, the high-energy spectral index is $\beta = -2.427 \pm 0.07$, and the break energy is $\epsilon_b = 149.5 \pm 2.1$.

1.10),

$$\frac{dN}{d\epsilon_\gamma} \propto \epsilon_\gamma^{-\alpha} \exp\left(-\frac{\epsilon_\gamma}{\epsilon_b}\right), \quad \epsilon_\gamma \leq (\beta - \alpha)\epsilon_b \tag{1.8}$$

and at high energy with a steeper power-law

$$\frac{dN}{d\epsilon_\gamma} \propto \epsilon_\gamma^{-\beta}, \quad \epsilon_\gamma \geq (\beta - \alpha)\epsilon_b, \tag{1.9}$$

in which $\beta > \alpha$ and ϵ_b is the break energy, i.e. the energy at which the spectrum breaks. This broken but smoothly-connected power-law is called the Band function, named after astronomer David Band who first-authored the paper discussing the energy spectra of BATSE GRBs (Band et al., 1993). It is necessary here to point out that the Band function is phenomenological in nature and is not physically motivated. Nevertheless it is without doubt very useful since it could fit well with a large number of GRB spectra and thus provide hints to the mechanisms of γ-ray emission.

The second notable BATSE result is the identification of two classes of GRBs based on their burst duration and hardness ratio. The now-standard method to determine the burst duration is to measure the time interval during which the integrated counts from the burst increase from 5% to 95% of the total counts (Kouveliotou et al., 1993). Such duration is called T_{90}. The distribution of T_{90} exhibits a bimodality suggesting two different classes of

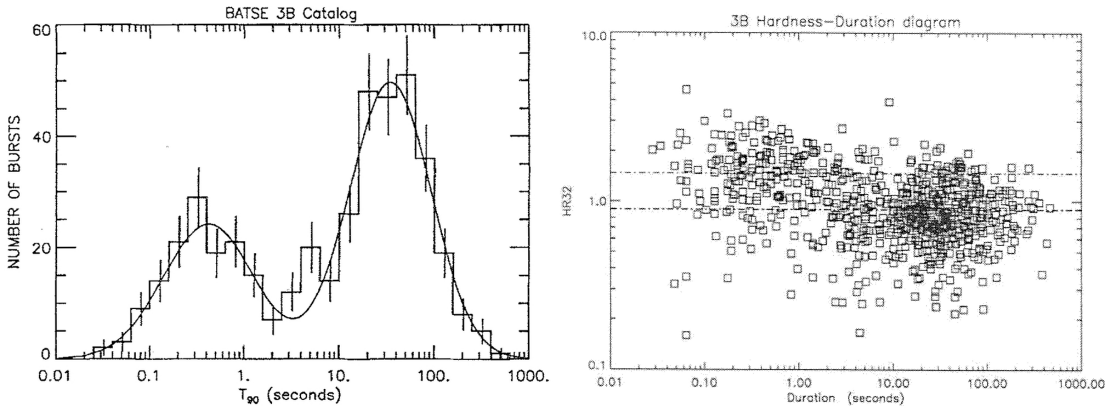

Figure 1.11: *Left:* The T_{90} distribution for GRBs from the BATSE 3B Catalogue, here reproduced from Kouveliotou et al. (1996). The solid line is a fitting of two log-normal distribution to the data. *Right:* The hardness ratio – T_{90} diagram for GRBs from the BATSE 3B, also reproduced from Kouveliotou et al. (1996). The dashed-dotted lines are the average hardness for the short (top line) and long (bottom line) GRBs, which is separated at 2 second.

GRBs: short-duration GRBs which typically last less than 1 second and long-duration GRBs which typically last more than 10 second (Kouveliotou et al., 1996, Figure 1.11, left). The demarcation between short and long GRBs is usually taken to be 2 second. We can also correlate T_{90} with what is known as the hardness ratio. Denoted as $HR32$, the hardness ratio is the ratio of the total count of a GRB during the T_{90} interval in the range of 100–300 keV with the total count between 50–100 keV. The correlation between $HR32$ and T_{90} shows that long GRBs are predominantly soft while short GRBs are predominantly hard (Kouveliotou et al., 1996, Figure 1.11, right).

An important event in GRB astronomy happened in 1997, when the first high-resolution X-ray images of a GRB were made for the first time by the Italian-Dutch satellite *BeppoSAX*[7] (Costa et al., 1997). Eight hours after the γ-ray detection of GRB 970228, a fading X-ray afterglow of the burst was discovered (Figure 1.12), which has been theoretically predicted (Mészáros & Rees, 1997). This leads to an arcminute-accuracy pinpointing of the GRB position, which allows us to perform follow-up observations in the longer wavelength. An optical observation of the afterglow would soon follow (van Paradijs et al., 1997) as well as the discovery of the first GRB afterglow in the radio band (Frail et al., 1997, GRB 970508). The discovery of the afterglow allows us to determine

[7] Satellite per Astronomia a raggi X. *Beppo* is the nickname of physicist Giuseppe Occhialini. `http://www.asdc.asi.it/bepposax/`

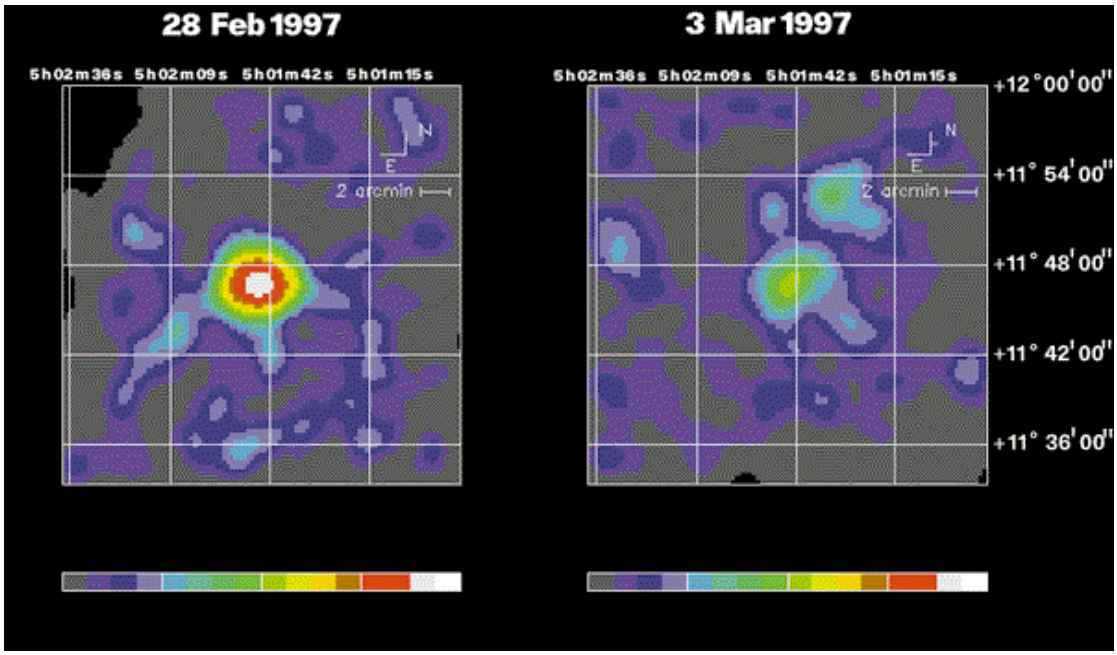

Figure 1.12: The discovery of the first X-ray afterglow of a GRB, 970228. These are false-colour images of the afterglow taken with the *BeppoSAX* Medium Energy Concentrator Spectrometer (2–10 keV). White corresponds to 31 counts per pixel^2, green corresponds to 6 counts per pixel^2, and grey to a background of 0–1 counts per pixel^2. Images reproduced from Costa et al. (1997).

their redshift, to identify the host galaxies, and to confirm their cosmological origin (Metzger et al., 1997). GRB astronomy has gone multiwavelength.

A MODEL of GRB has appeared even before their actual detection, when Colgate (1968, 1974) proposed the very first model of a γ-ray burst. In this model, prompt γ-rays and X-rays could be emitted as the breakout of relativitistic shocks from the photosphere of supernovae (SNe). The lack of GRB-supernova connection was however noted by Klebesadel, Strong & Olson (1973), who pointed out that there were no observed supernovae within several weeks around the time of the bursts. They did however aware that numerous supernovae could occur undetected if it is too faint in the optical regime.

The idea of GRB-SNe connection resurfaced time and again (e.g. Paczyński, 1986), but it was not firmly established until much later, in 1998, when GRB 980425 occurred in conjunction with SN 1998bw. The GRB was detected both by *BeppoSAX* (Soffitta et al.,

1998) and BATSE. Within the 8'-radius error circle lies a late-type galaxy ESO184-G82 (z = 0.0085, Tinney et al. 1998), hosting in one of its spiral arm a luminous supernova designated 1998bw (Sadler et al., 1998). Initially the association of the GRB with the SN was controversial, but follow-up observations by *BeppoSAX* reveal a variable X-ray source at the location of the SN (Pian et al., 2000). Further *Chandra* observations of the location increase the confidence in the connection between the GRB and the SN (Kouveliotou et al., 2004).

On the surface, the GRB looks unremarkable. It has a smoothly-broken power law with break energy $\epsilon_b = 148$ keV and a moderate burst duration that last $T_{90} = 23.3$ s (Galama et al., 1998). However GRB 980425/SN 1998bw was quite unusual for a GRB because its redshift implies an underluminous γ-ray energy output, having an isotropic emission of $L_\gamma = 8 \times 10^{47}$ erg (Galama et al., 1998). This is more than three orders of magnitude fainter than a typical long-duration GRB, which is at the order of 10^{52} erg (Butler, Bloom & Poznanski, 2010), and any collimation into jets would make the energy output in γ-ray even smaller. This unusual property led to the consensus that GRB 980425/SN 1998bw is an example of one extreme end of a spectrum of events with the same underlying physical mechanism (Woosley & Bloom, 2006), and the notion that GRBs are associated with SNe is maintained. The first unambiguous association of a GRB with a Supernova came later when HETE[8] satellite (Ricker et al., 2003) detected GRB 030329/SN 2003dh (Hjorth et al., 2003).

The large redshifts of GRBs imply that the isotropic γ-ray fluences are of the order of one solar rest mass, $M_\odot c^2 \sim 2 \times 10^{54}$ erg, which is $\sim$1000 times the total energy emitted by a typical SN (Mészáros, 2006). This huge energy requirement could be reduced significantly, however, if the emission is collimated into a jet. Observations of breaks in the optical and IR light curves of the GRB afterglows show that this is indeed the case (Kulkarni et al., 1999; Castro-Tirado et al., 1999). This collimation would then make the total energy output comparable to that of SNe, the difference being that the energy of GRBs is emitted mostly in γ-ray over a very short period of tens of seconds, while SNe emit their energy isotropically mostly in the optical wavelengths over longer period

GRBs are designated by the date of their detection. In this way, GRB 980425 is the burst that has been detected on April 25 1998. If more than one burst is detected during the day, a letter is appended to the name: GRB 980425A, for example, is the first GRB detected on April 25 1998, GRB 980425B is the second, and so on. The same naming convention also applies to supernovae, except that only the year is used to name the supernova, e.g. SN 1998, which means that the supernova is detected in 1998. Capital letters from A to Z are appended to indicate the order of detection in that year, followed by pairs of lower-case letters after all the letters of the alphabet has been used. Hence SN 2005nc is the 367th supernova discovered in 2005.

[8] High Energy Transient Explorer, `http://space.mit.edu/HETE/`

of several weeks.

The small time variability δt of GRBs, which is at the order of miliseconds, implies typical emitting regions of several thousand kilometers, i.e. $c\delta t = 3000\ \mathrm{km}(\delta t/10\ \mathrm{ms})$. Within this very small space, around 10^{51}–10^{53} erg of energy—which is more than the total emission of the Sun during its lifetime—must be injected within a few tens of seconds. The sudden release of this large amount of energy will result in the conversion of a fraction of this energy into neutrinos and gravitational waves, and a significantly smaller fraction $(10^{-3}$–$10^{-2})$ is converted into a fireball composed of baryons, $e^{\pm}$, and γ-rays. This fireball is transparent to gravitational waves as well as to neutrinos (Mészáros, 2006).

Observations suggest that the photon luminosity of the fireball is many orders of magnitude larger than the Eddington luminosity $L_E = 4\pi GMm_p c/\sigma_T = 1.25 \times 10^{38}(M/M_\odot)$ erg s^{-1}, which means that the radiation pressure of the fireball exceeds its self-gravity and thus should expand. However, the injection of so much energy into a very small space within a very short time implies that the fireball should be very opaque to high-energy photons. Photons with MeV energy and higher would annihilate to create electron-positron pair. Consequently we should not observe high-energy γ-rays, yet we do. The energy spectrum of GRBs extend to MeV (Matz et al., 1985; Schneid et al., 1992) and occasionally also observable to the GeV regime (Abdo et al., 2009). To solve this compactness problem, first the total mass of baryons in the central region of the progenitor must be below $\sim 10^{-12} M_\odot$ so that the electrons do not produce a large opacity (Paczynski, 1990), and second the fireball must expand relativistically so that the baryon density decrease rapidly and thus the opacity to photon-photon collisions could be avoided.

The energy threshold for two photons to annihilate and create a pair of electron-positron is $\epsilon_{\mathrm{th}} = m_e c^2 = 0.511$ MeV

The relativistic expansion of the fireball solves the compactness problem in three ways. Suppose the fireball expands relativistically with a bulk Lorentz factor Γ. The observed photons will then be blueshifted by a factor Γ, so that the observed γ-rays are actually X-rays in the fireball. This greatly reduces the number of photons at the fireball that is actually above the pair-production threshold. Secondly, for a typical observed timescale of δt, the

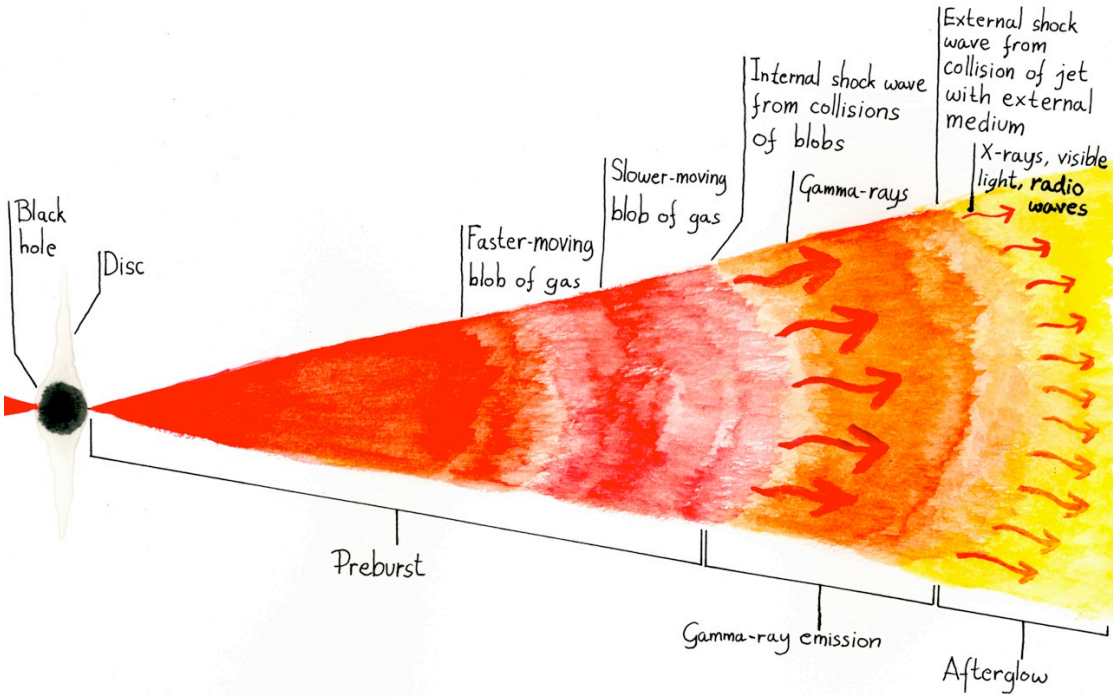

Figure 1.13: An illustration of the various phases in the GRB standard model, with the internal and external shocks and the radiations they emit. Illustration by the author, based on an illustration by Juan Velasco in Gehrels, Piro & Leonard (2002).

physical size of the emitting region is actually $\Gamma c\delta t$ instead of $c\delta t$ for a stationary source, which means that the density of photons is reduced considerably. Thirdly, relativistic beaming implies that only a small fraction $1/\Gamma$ of the source is observable, regardless of the opening angle of the jet. This means that the relative angle of the photon-photon collisions must be less than the Γ^{-1}, which also reduces the effective rate of pair-production for a large Γ.

These three combined effects reduce the optical depth for pair creation by a factor $\Gamma^{2+2\alpha}$, where α is the spectral index of the observed photon spectrum, $dN_\gamma/d\epsilon_\gamma \propto \epsilon^{-\alpha}$. For $\alpha \sim 2$ this would mean a drop of optical depth by a factor of Γ^6 (Zhang & Mészáros, 2004). Considering these effects, for $\alpha \sim 2$ it is found that $\Gamma \geq 100$ is required in order that the pair-production optical depth is less than unity (Piran, 1999; Lithwick & Sari, 2001).

Evidence for the relativistic expansion of the fireball is provided by radio observations of the GRB afterglow, which shows a strong

irregular variations in the radio flux that dampened after about a month. These variations are caused by the interstellar scintillation in our Galaxy. The damping of the fluctuations afterwards reflects the increasing size of the source. By knowing the distance to the source and the properties of the insterstellar medium along the line of sight, the size of the source by the time the fluctuations disappear could be determined. Frail et al. (1997) employed this method to GRB 970508 and found out that the radio afterglow expanded with velocity close to the speed of light.

It is inside and around this relativistically expanding fireball that the γ-ray emission we observe is produced, through internal shocks (Rees & Mészáros, 1994) and external shocks (Rees & Mészáros, 1992). Inside the fireball, time-varying outflow from the GRB central engine leads to successive shells of materials ejected with varying Lorentz factor (Figure 1.13). A fast blob ejected after a slower one will eventually overtake and collide with it. Due to the relativistic expansion of the fireball, the timescale that we observed is compressed by a factor Γ^{-1}. Thus the γ-ray burst that we observe in only a few seconds could actually take a day to produce. These shocks can thus explain the rapidly varying light-curves of the prompt γ-ray emission.

As the fireball expands and eventually slows down, it collides with the external medium surrounding the GRB, forming an external shock wave that will persist even as the fireball slows down. This type of shock explains quite well the GRB afterglow emission and its gradual degradation from γ-rays to X-rays to visible light and finally to radio waves. A reverse shock that propagates back into the fireball can also occur. As the reverse shock crosses the fireball, it will heat up the matter in the fireball and accelerates electrons, producing a strong optical flash and a radio flare (Mészáros & Rees, 1997).

THE PROGENITOR that becomes the central engine of a GRB is thought to involve compact objects at its heart. It is natural to think this way because of the small time variability which implies a progenitor possessing huge energy occupying a very small volume. The nonrepetition of a GRB means that the progenitor is catastrophically destroyed.

One family of progenitor models, called the hypernova or collapsar model, involves rotating massive stars with $M_* \gtrsim 20 M_\odot$. In this model the iron core of such star will eventually collapse, forming a black hole encircled by a debris disk (Woosley, 1993; Popham, Woosley & Fryer, 1999; MacFadyen & Woosley, 1999). Within minutes following the collapse, the black hole accretes the residual matter into the center and funnels them into a powerful relativistic jet that will be observed as a GRB if the jet happens to point towards the Earth. The massive star must also have shed its hydrogen-rich envelope at the time of collapse, in order to not only avoid a significant amount of baryon-loading into the jet, but also to allow the jet, which is formed deep inside the star, to break through the body of the star and develops.

Numerical simulations of collapsars show that the progenitors can not produce bursts shorter than $\sim$5 s (MacFadyen & Woosley, 1999). We observe nevertheless short-hard bursts in Figure 1.11, so their existence require other kind of progenitors. The merger of a compact binary could explain this.

There are many variations within the merger of compact binary scenario: a neutron star merges with another neutron star (NS-NS), black hole + neutron star (BH-NS), black hole + white dwarf (BH-WD), or black hole + helium star (BH-He).

The merger of two neutron stars provide a huge supply of gravitational binding energy that can be channeled into the fireball, and a baryon-clean region along the rotation axis of the binary. The fireball is created from the enormous compressional heating and dissipation associated with the accretion. The relativistic expansion of the fireball is driven by $\nu\bar{\nu} \rightarrow e^+e^-$ annihilation or strong magnetic fields in at the order of 10^{14} G (Rosswog, Ramirez-Ruiz & Davies, 2003). A black hole will be formed from the NS-NS merger, while remnants of the merger form a neutron-rich high-density torus that will orbit the black hole. Neutrinos and antineutrinos from the torus then annihilate to produce an ultrarelativistic e^+e^- plasma outflow along the rotation axis, which becomes the fireball.

The torus is very dense and thus only neutrinos can extract its thermal energy present in the torus. The neutrino emission will be focused along the original binary rotation axis, as the pole regions

are covered with high-density walls of the thick disk and the steep density gradient in the radial direction prevents lateral expansion. In a particularly baryon-clean region, a relativistic outflow can be accelerated by $\nu\bar{\nu}$ annihilation. While it is similar to the collapsar mechanism suggested by MacFadyen & Woosley (1999), in this case the jet does not have to burrow through the stellar envelope.

The typical isotropic energy provided by the $\nu\bar{\nu}$ annihilation is $E_{\rm iso} \sim 10^{48}$ erg, emitted within 0.2 second after the merger (Rosswog, Ramirez-Ruiz & Davies, 2003). This is comparable to the typical duration of a short-hard burst. Gravitational wave emission is also expected from short-hard bursts (Cutler & Thorne, 2002).

THE EXTENSION of the Band spectrum to the megaelectronvolt (MeV) regime has been observed even before the launch of *Compton*. The Solar Maximum Mission[9] (SMM) and the Franco-Soviet PHEBUS detector on the *Granat*[10] mission has detected GRBs with γ-ray energy up to 10 MeV (Matz et al., 1985; Barat et al., 1992). These authors showed that the spectra of GRBs very often extend to this high-energy regime, while on the other hand the observations of γ-ray emissions up to 100 MeV have only been reported for a small number of GRBs, mainly by the COMPTEL[11] and EGRET instruments on board the CGRO (Schneid et al., 1992; Hanlon et al., 1994; Winkler et al., 1995; Kippen et al., 1998). Between 1991 and 1995 COMPTEL observed 29 GRBs in the range 0.75–30 MeV and suggested that GRB spectra extend at least to hundreds of MeV.

Observations in the gigaelectronvolt (GeV) regime has been reported only for a handful of GRBs. EGRET observed seven GRBs with emissions in the MeV and GeV regime (Kwok et al., 1993; Hurley et al., 1994; Sommer et al., 1994; Dingus, 1995). Particularly interesting is GRB 940217 which lasted for 90 minutes and includes an emission of an 18 GeV photon emitted ∼4500 s after the low-energy emission has ended (Hurley et al., 1994). The launch of *Fermi*[12] in 2008 provides an opportunity to observe the GeV part of GRB spectra since one instrument on board *Fermi*, the Large Area Telescope[13] (LAT), is particularly sensitive to GeV γ-rays. The LAT is a pair-conversion telescope that measures the

[9] http://heasarc.nasa.gov/docs/heasarc/missions/solarmax.html

[10] http://heasarc.gsfc.nasa.gov/docs/granat/granat.html

[11] Imaging *Compton* Telescope, http://heasarc.gsfc.nasa.gov/docs/cgro/comptel/

[12] *Fermi* was formerly named GLAST (Gamma-ray Large Area Space Telescope) before NASA invited the general public to suggest a new name for it. http://fermi.gsfc.nasa.gov/

[13] http://www-glast.stanford.edu/

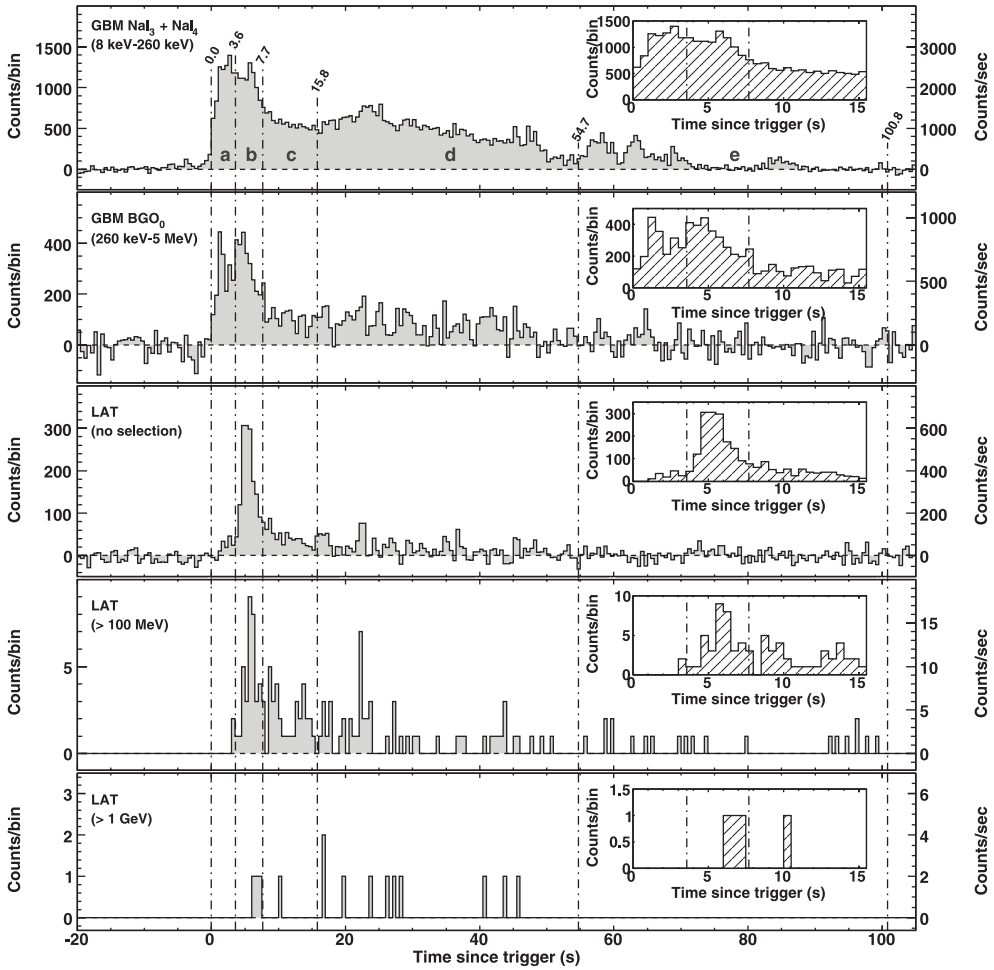

Figure 1.14: The light curves of GRB 080916C observed with the GBM and the LAT, from the lowest to highest energies. The Figure is reproduced from Abdo et al. (2009).

tracks of the electron (e^+) and positron (e^-) that result when an incident γ-ray passes through the detector and undergoes pair-conversion. It is sensitive to γ-rays with energies between 20 MeV–300 GeV, and has an effective area of 0.95 m^2 for γ-rays coming at normal incidence (Atwood et al., 2009). On September 16 2008, an exceptionally bright GRB triggered the Gamma-Ray Burst Monitor[14] (GBM) instrument onboard *Fermi*. Both GBM and LAT observed the GRB and extract the light curve of the GRB at various energy ranges (Abdo et al., 2009). Fourteen events were observed to have energies in excess of 1 GeV and the highest observed γ-ray

[14] `http://gammaray.msfc.nasa.gov/gbm/`

energy is $\sim$13 GeV. What is particularly interesting with the observation of this GRB is that the peak of the emission is shifted as we move to higher energy regime (Figure 1.14). One way to explain this shift to the higher energy is by invoking a hadronic model associated with ultra-high energy cosmic-ray (UHECR). The delay of the emission is simply the consequence of the time required to accelerate protons into higher energies where they can generate an electromagnetic cascade either by photopion or by proton synchrotron radiation (Abdo et al., 2009). This could be one of the major clues on the emission mechanism of GRBs.

Moving further to the teraelectronvolt (TeV) regime, up to the time of writing there is still no firm evidence of TeV γ-ray emission from GRBs, but not for the lack of trying. Attempts have been made to detect TeV components of GRBs. Using coordinates distributed by the BATSE Coordinates Distribution Network (BACODINE) and later on by the GRB Coordinates Network (GCN), the *Whipple*[15] collaboration has observed 9 BATSE GRBs and 7 other GRBs announced by GCN within minutes to hours after the burst time given by the alert (Connaughton et al., 1997; Horan et al., 2007). No evidence of TeV emission were found but upper limits were reported. The MAGIC[16] Telescope, using the same observation principle as *Whipple*, observed 9 GRBs announced by GCN and found no evidence of TeV emission as well (Albert et al., 2007).

So far the only indication of TeV emission were detections by the HEGRA[17] AIROBICC[18] detector who claimed $\gtrsim$ 16 TeV emission from GRB 920925c (Padilla et al., 1998), the *Milagrito*[19] collaboration (Atkins et al., 2000b, 2003, 2005) who reported detection of γ-rays at $\sim$650 GeV, and the GRAND[20] array (Poirier et al., 2003) at 0.01 TeV. The observations by *Milagrito* and GRAND will be described below.

Milagrito is a water Čerenkov array of size $35 \times 44 \times 2$ m at an altitude of 2650 m near Los Alamos, New Mexico, United States. It comprise 228 photomultiplier tubes arranged in a 2.8×2.8 m grid, submerged in a large pool of water with volume 24×10^6 liter (Atkins et al., 2000a). *Milagrito* operated in 1997–1998 and was later replaced by *Milagro* which has better sensitivity. During the period of *Milagrito*'s activity, 54 BATSE GRBs were observed but

[15] http://www.sao.arizona.edu/FLWO/whipple.html

[16] Major Atmospheric Gamma-ray Imaging Čerenkov, http://wwwmagic.mppmu.mpg.de/

[17] High-Energy-Gamma-Ray Astronomy, http://www.mpi-hd.mpg.de/hfm/HEGRA/HEGRA.html

[18] AIRshower Observation By angle Integrating Čerenkov Counters

[19] A prototype of the *Milagro* Gamma-ray Observatory, http://www.lanl.gov/milagro/index.shtml

[20] Gamma Ray Astrophysics at Notre Dame, http://www.nd.edu/~grand/

Milagro is Spanish for *miracle*, while its aptly-named smaller predecessor *Milagrito* is the diminutive form of *milagro*.

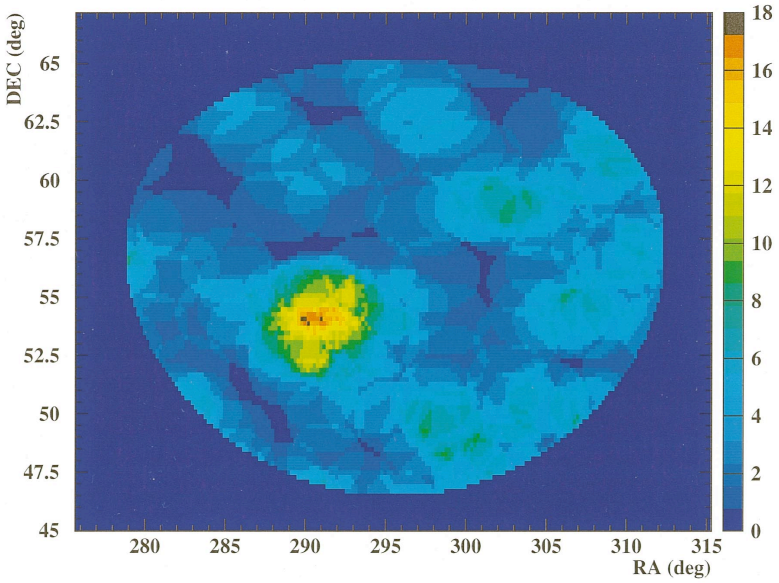

Figure 1.15: *Milagrito* observation of TeV γ-ray emission from GRB 970417A, here reproduced from Atkins et al. (2000b). The plot shows the number of events recorded during the T_{90} duration in overlapping 1.6° radius bin within vicinity of the GRB.

only one, namely GRB 970417A, exhibits an excess of events over background (Atkins et al., 2000b). The probability that such an excess is caused by background fluctuation is 2.8×10^{-5} (Figure 1.15), however this increases to 1.5×10^{-3} if we take into account the fact that all 54 GRBs were observed. Further analysis indicate that this excess over background must be caused by γ-rays with energies of at least 650 GeV (Atkins et al., 2003). If this excess is true then it can be implied that the total isotropic energy of the GRB in the TeV range is $\sim 10^3$ times than the total isotropic energy in the MeV (Totani, 2000). One interpretation of this phenomenon is through the proton-synchrotron model, in which only $(m_e/m_p) \sim 10^{-3}$ of the kinetic energy of the fireball is carried by electrons and the rest is carried by protons. If this energy carried by the protons is then emitted as γ-rays, much more energy could be radiated in the TeV regime than the sub-MeV range by a factor of $\sim$1000 (Vietri, 1997; Totani, 1998a,b, 1999).

GRAND is a muon detector array located north of the University of Notre Dame campus, approximately 150 km east of Chicago, Illinois, United States. It detects γ-ray-induced muons

at ground level by employing 64 tracking stations of proportional wire chambers (PWC). GRAND has a collecting area of $\sim$80 m^2. Eight GRB candidates were observed by GRAND and one of them, GRB 971110, showed an excess of 466 ± 171 muons during its BATSE T_{90} interval. The probability that this excess is caused by background fluctuation is 3×10^{-3}, or 0.025 probability to observe such background fluctuation in one of the eight bursts observed by GRAND. The detection significance of GRB 971110 is therefore marginal at 2.7σ (Poirier et al., 2003).

Another attempt to detect TeV γ-ray was done by the Tibet ASγ Experiment[21]. It is a Sino-Japanese experiment located in Yangbajing, Tibet, at 4300 m above sea level. Tibet ASγ consists of 221 scintillation counters with area 0.5 m^2 each and are placed on a 15 m^2 grid. Using the scintillation detector array, Tibet is able to observe the extensive air shower induced by not only cosmic rays but also by γ-rays. With a duty cycle of 24 hours per day regardless of weather condition and a wide field of view of about 2 steradian, Tibet ASγ provide an unbiased survey of TeV sources in the northern sky (Amenomori et al., 2010). They have succesfully observed γ-ray sources in the TeV range, such as the Crab Nebula (Amenomori et al., 1999), Markarian 501 (Amenomori et al., 2000), and Markarian 421 (Amenomori et al., 2003). Between October 1995 and March 1996, data coincident with 69 BATSE GRBs were analysed, in search of multi-TeV signals. No significant TeV γ-rays were discovered (Amenomori et al., 2001).

[21] AS stands for *air shower*. http://www.icrr.u-tokyo.ac.jp/em/

We can see that there are very little results from the search of TeV γ-ray emission from GRBs, but nevertheless the question of whether GRBs emit TeV γ-rays is an important one, as the observations or the lack thereof TeV γ-rays from GRBs would provide important constrains on the acceleration mechanisms of cosmic rays. One of the more specific big questions in GRB astronomy is whether the jets of GRBs are dominated by ultrarelativistic protons or pairs of e^+e^-. We have seen that protons are an important component in producing TeV γ-rays, and thus the observation of TeV γ-ray emissions from GRBs is an important clue in answering these questions.

1.3 *Teraelectronvolt astronomy: tools of the trade*

IT CAN be said that TeV γ-ray astronomy is the "final frontier" in photon astronomy, as it is the last electromagnetic window to be opened (Aharonian, 2004). Whereas photons with energies lower than X-ray are mostly emitted by thermal processes and exhibit blackbody spectrum, photons with energies at the X-ray regime and above are emitted through nonthermal and relativistic processes. Their power-law spectrum also confirms their nonthermal origins.

To observe γ-ray photons is then to observe the most extreme part of the universe. These energetic phenomena are of particular interest to particle physicists as they involve natural accelerators and physical processes that are difficult, if not impossible, to emulate in laboratories. It is a small wonder then that the first γ-ray astronomers generally came from high-energy particle physics community interested in energetic phenomena in the universe (Weekes, 2003). γ-ray astronomy as a concept was first put forward by Morrison (1958). In his seminal 1958 paper, he not only described the physical process that could produce cosmic γ-rays but also outlined the methods to detect them and list a number of possible γ-ray sources.

The γ-ray regime covers at least 14 decades in energy. It spans from approximately the energy of an electron, $E = m_e c^2 \approx 0.5 \times 10^6$ eV to $\geq 10^{20}$ eV. This lower bound corresponds to the region of nuclear γ-ray lines as well as the electron-positron annihilation line, while the upper bound corresponds to the highest observed energy of cosmic rays (Aharonian, 2004). We can divide this wide energy band into several areas defined somewhat arbitrarily: the *low* energy (LE, below 30 MeV), *high* (HE, 30 MeV–100 GeV), *very high* (VHE, 100 GeV–100 TeV), and *ultra high* (UHE, beyond 100 TeV). This subdivision has little to do with the physical processes involved in their radiation but has more to do with the interaction phenomena of γ-rays with matter and the various techniques employed for their detection.

Observations in the low and high-energy band are carried out by space satellites or balloons in the upper atmosphere. In the LE regime the Compton process is the dominant interaction mode

used for the detection. Detection in the HE and VHE regime makes use of the pair-production interaction but in different ways: balloons or spaceborne HE telescopes employ spark chambers to identify the electron-positron pair produced as γ-rays interact within the spark chamber plates. On the other hand, ground-based VHE detectors detect the electromagnetic showers that develop in the Earth's atmosphere as γ-rays interact with the atmosphere.

Even though spark chambers have been obsolete for high-energy physics experiments, they have long been the workhorse detector in HE γ-ray astronomy and has been employed to great success among others by EGRET.

It is readily apparent that there are certain peculiarities unique to γ-ray astronomy that are not present at lower energy regimes. In other regimes of the electromagnetic spectrum, astronomical telescopes take advantage of the fact that light passing through a large aperture can be concentrated to a much smaller area through reflection of refraction, making the size of the detector just a small fraction of the telescope aperture. Optical, infrared, radio, and even X-ray astronomers take advantage of this fact and design a suitable geometry to concentrate photons into a small detector element, so that the signals are detectable above a certain background.

The penetrating power of γ-rays at MeV energies and above prevents them to be efficiently reflected off a surface and thus nuclear physics detection methods must be employed to observe the interaction of γ-rays with matters. In general, the size of a γ-ray "telescope" is then effectively only as big as the size of the detector itself (however, as we shall see later on, this will not be the case for ground-based VHE γ-ray telescopes). It is also necessary to identify cosmic γ-ray events from the charged particle backgrounds. Payload constraints must also be taken into account for spaceborne telescopes. *Compton* was one of the largest and heaviest scientific instruments ever put into space and yet its LE telescope, COMPTEL, and its HE telescope, EGRET, had effective apertures of respectively 5 cm^2 (Diehl, 1988) and 2000 cm^2 (Kanbach et al., 1988).

The second peculiarity of cosmic γ-ray detection is that the Earth's atmosphere is opaque to all γ-rays. Even on top of the highest mountains it is still many radiation lengths below the top of the atmosphere, thus it is virtually impossible to directly detect

γ-rays without sending instruments to outer space. Balloons can lift γ-ray detectors to near the top of the atmosphere and much of the pioneering works in γ-ray astronomy was done this way. Later on as rocket technology improves, satellites operating high above the atmosphere can carry heavier γ-ray detectors. The absorption of γ-rays by the atmosphere, however is not without its own merit, as their interaction will produce a cascade of charged particles that could be detected by dedicated instruments.

Not long after the publication of Morrison's paper on γ-ray astronomy, Cocconi published an optimistic prediction for VHE γ-ray astronomy and suggested a design of a VHE γ-ray telescope consisting of arrays of particle detectors (Cocconi, 1960). This method has been succesfully applied to detect cosmic ray showers, however other experimenters realized that for γ-ray-induced cascade a higher sensitivity could be gained by detecting instead the Čerenkov radiation. A group of Soviet physicists from the Lebedev Institute then build an array of 12 light detectors in the Crimea, and after four years of observing the sources suggested by Cocconi (radio galaxies and supernova remnants) no convincing detection was made (Chudakov et al., 1967).

THE EARTH'S atmosphere is opaque to all electromagnetic radiation with energy greater than 10 eV. The vertical thickness of the atmosphere above sea level is approximately 1030 g cm^{-2}. Since one radiation length in air is $X_0 = 36.62$ g cm^{-2} (Nakamura & Particle Data Group, 2010), the thickness of the atmosphere is equal to more than 28 radiation lengths. While the γ-ray itself may be absorbed by the atmosphere, the secondary products of its interaction with the atmosphere do survive and are detectable.

The dominant interaction of a γ-ray with energy greater than 10 MeV is pair-production. Typically this will occur after one radiation length has been traversed. The resulting electron-positron pair will share the energy of the parent γ-ray and will be emitted in virtually the same direction as the original direction of the γ-ray. After this pair traverse another radiation length, they could interact with the atmosphere to emit secondary γ-rays through bremsstrahlung. A secondary γ-ray could also produce another electron-positron pair after another radiation length. This pro-

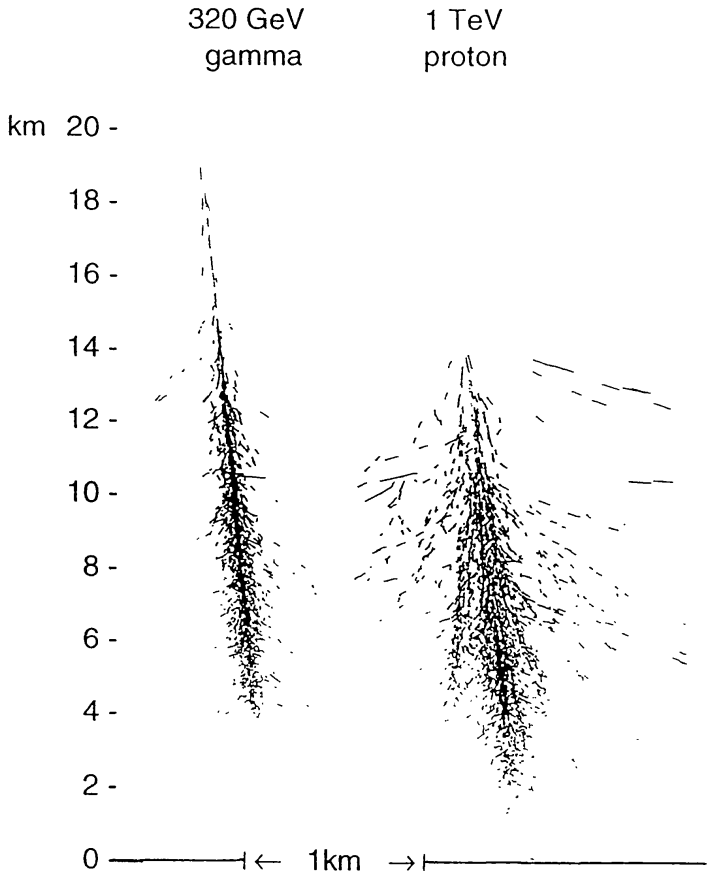

Figure 1.16: Monte Carlo simulations of a 320 GeV γ-ray shower and a 1 TeV proton shower. The horizontal scale is exaggerated by a factor of 5. Figure reproduced from Hillas (1996).

cess continues down through the atmosphere (Figure 1.16) until the average energy of the particles drops to a point where ionization energy losses and the radiation losses become equal (Rossi & Greisen, 1941). At this point the shower reaches a maximum and the number of particles gradually diminishes and the cascade dies away.

If the energies of the secondary electron-positron pairs are above the Čerenkov threshold, i.e. they travel with velocities above the velocity of light in the atmosphere, they will make the atmosphere radiate Čerenkov photons. Since many of the electron-positron pairs will be above the threshold, the cascade will also be accompanied by a shower of Čerenkov photons. As the refractive index

The Čerenkov threshold for the atmosphere is 21 MeV at sea level. The Čerenkov angle at sea level is $\theta_c \sim 1.3^\circ$ where the refractive index is n = 1.00029.

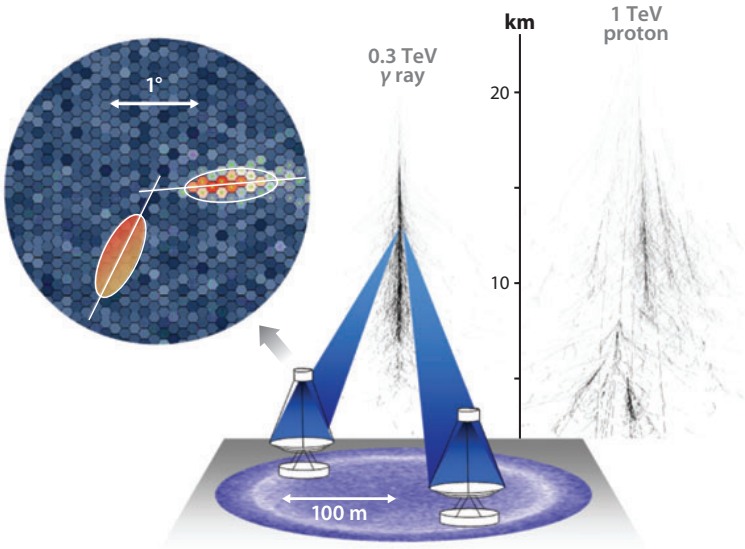

Figure 1.17: An illustration describing the method to detect VHE γ-rays using ground-based optical reflectors. As γ-rays interact with the Earth's atmosphere, they will produce pairs of electron-positron that will make the atmosphere radiate Čerenkov photons. With ground-based telescopes one could detect these photons and reconstruct the direction and energy of the γ-rays. Because the secondary radiation arrives at detector level as a broad but thin disk, the detector can have a large collecting area for the primary γ-ray detection. The formation of an image on the camera of a Čerenkov telescope is also shown. Illustration reproduced from Hinton & Hofmann (2009).

of air is close to unity, the shower will point in the forward direction. From an observer on the ground, the shower of Čerenkov photons will look similar to meteoric trails (Weekes, 2003). If the trails are extrapolated backward they will point back to their origin. A simple reflector equipped with photomultiplier tubes and a fast pulse-counting electronics could in principle detect the cascade (Figure 1.17) and determine the point of origin, energy, and the time of arrival of the γ-ray. Thus a map of VHE γ-rays could be produced, the energy spectrum be determined, and variability of the source could be measured.

The unique feature of atmospheric Čerenkov telescopes (ACT) is that the telescope can have a large collecting area for the detection of the primary γ-rays, beyond of the size of the mirror area itself. This is because the secondary radiation arrives at detector level as a broad but thin disk (Figure 1.17). Since the radius of the Čerenkov light pool on the ground could reach $\sim$120 m, the shower detection area is $\sim 5 \times 10^4$ m^2 (Weekes, 2003), which is huge by astronomical standards. Since at high-energies the fluxes of cosmic γ-ray are low, this large collecting area is a key advan-

tage compared to spaceborne γ-ray detectors.

The main limitation of ACTs is that they can only operate with a low duty cycle, because the photomultiplier tubes are sensitive to stray background lights such as moonlight, starlights, airglow, lightning and meteoric trails, and manmade light sources such as satellite lights and airplanes. By building the telescope away from human habitations, manmade background lights could be avoided. By choosing the observing time, natural background lights such as the Sun, Moon, and lightning could be avoided. To minimize the natural background due to starlight and airglow, it is best to choose the photomultipliers with higher quantum efficiency in the blue light, which is the peak emission of the Čerenkov photons (Weekes, 2003). As a consequence of these limitations, ACTs can only operate $\sim$1000 hours per year (Hinton & Hofmann, 2009). This corresponds to a duty cycle of $\sim$10%. Other limitations of ACTs are their narrow field of view, which is typically $\sim5^\circ$ (Hinton & Hofmann, 2009), and their slow slewing capability toward an intended target. The shortest slewing time is $\sim$80 s for MAGIC (Albert et al., 2007).

Despite the huge collecting area and high sensitivity, the low duty cycle and the long slewing time make ACTs a limited instrument to observe GRBs. As we have discussed in the previous section, efforts were made by ACTs to observe GRBs but no significant signals were found. On the other hand, for the observations of steady sources such as supernova remnants and active galactic nuclei, ACTs have been proven to be the most powerful instrument to study these objects.

THE FIRST large optical reflector built to observe atmospheric Čerenkov radiation was the *Whipple* 10 m γ-ray telescope installed on Mount Hopkins in southern Arizona in 1968. It was not until 1989 that *Whipple* finally made the first robust detection of VHE γ-rays, the Crab Nebula (Weekes et al., 1989). Since then numerous other Čerenkov telescopes have been built and today $\sim$80 VHE γ-ray sources have been identified (Hinton & Hofmann, 2009).

Over time, the Crab Nebula has become the "standard candle" of high-energy astrophysics. Fluxes of high-energy sources are customarily measured in units of the Crab's flux.

The performance of ACTs can be significantly improved if multiple telescopes are employed so that the shower could be imaged

Instrument	Lat. [°]	Long. [°]	Alt. [m]	Tels.	Area [m^2]	Pixels/ camera	FoV [°]	Thresh. [TeV]	Sens. [% Crab]
HESS	-23	16	1800	4	428	960	5	0.1	0.7
VERITAS	32	-111	1275	4	424	499	3.5	0.1	0.7
MAGIC	29	18	2225	2	468	1039	3.5	0.03	1.0
CANGAROO	-31	137	160	3	172	427	4	0.4	15
Whipple	32	-111	2300	1	75	379	2.3	0.3	15

Table 1.1: Properties of several currently-active ACTs, compiled from Hinton & Hofmann (2009). The mirror area is the combined area of all telescopes.

from different viewing angles. The telescope separation must be large enough so that the baseline is long enough for stereoscopic imaging, yet small enough that multiple telescopes can still fit within the Čerenkov light pool (Figure 1.17). This stereo detection could improve angular resolution as well as the rejection of backgrounds due to cosmic-ray induced showers. The availability of multiple images of the same shower allows for a reduction of the energy threshold by using a coincident trigger between telescopes, a determination of shower maximum, and better angular resolution. The advantages of this system is first demonstrated by HEGRA, an Armenian-German-Spanish collaboration and the precursor of the MAGIC collaboration, with five ACTs installed on La Palma, Canary Islands (Konopelko et al., 1999). Most of the current generation of ACTs employ this stereoscopic system (Table 1.1). Telescopes such as HESS[22] can measure the direction of a single γ-rays with resolution of 3–6 arcminutes, an energy resolution of around 15%, and a cosmic-ray rejection factor of 1% or better. This allows the detection of sources as faint as 1% the strength of the Crab Nebula ($\nu F_\nu \sim 3 \times 10^{-13}$ erg cm^{-2} s^{-1} at $\sim$1 TeV) within 25 hours close to the zenith (Hinton & Hofmann, 2009).

[22] High Energy Stereoscopic System, `http://www.mpi-hd.mpg.de/hfm/HESS`.

The next generation of atmospheric Čerenkov telescope, the Čerenkov Telescope Array (CTA)[23], is currently in a preparatory phase. It is foreseen that it becomes operational with full capacity in 2018 (Actis et al., 2011). With CTA (Figure 1.18) an in-depth study of individual sources as well as a wide-field survey can be made. By employing telescopes of different mirror area, CTA is also expected to cover a wide energy band ranging from below 100

[23] `http://www.cta-observatory.org`

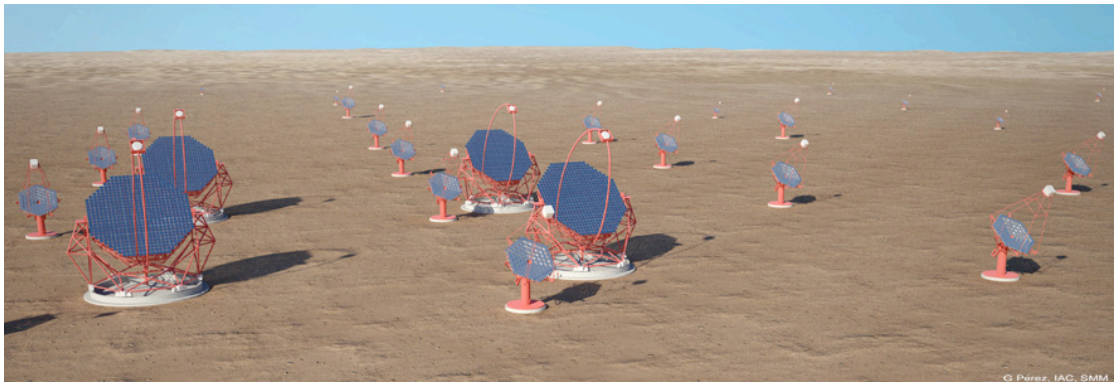

Figure 1.18: An artistic impression of the Čerenkov Telescope Array (CTA), currently in the preparatory phase and is expected to be fully operational in 2018. Credit: G. Perez, SMM, IAC, http://www.cta-observatory.org

GeV to more than 10 TeV. A small number of very large telescopes, possibly four, with a 20–30 m diameter will be used to detect γ-rays of energies below 100 GeV. The so-called core energy range between 100 GeV to 10 TeV will be covered by a grid of telescopes with 10–15 m diameter spaced $\sim$100 m apart. The high-energy range above 10 TeV may be detected by a large number of small telescopes with diameter of a few meters spaced within the size of the Čerenkov light pool. CTA is planned to be built on two separate sites. A main site to be located in the southern hemisphere covering an area of 3 km^2 will observe the central region of the Milky Way. A complementary northern site covering an area of 1 km^2 will be devoted to extragalactic studies such as the observation of AGNs and GRBs.

Despite the low-duty cycle of CTA, its expected sensitivity is 1% Crab in the wide-field survey mode. The fast-slewing capabilities will be used to observe GRBs in their afterglow phase or even earlier in their prompt phase. In a recent simulation of follow-up GRB observations with CTA, Kakuwa et al. (2011) conclude that CTA could observe $\sim$0.1 GRBs per year during the prompt phase and $\sim$0.5 GRBs per year during the afterglow phase. It is possible that a fraction of these observed GRBs could also be observed in the TeV regime.

A COMPLEMENTARY method of VHE γ-ray detection can be performed by directly detecting the air-shower particles. This re-

quires an array of a large number of particle detectors through which some of the particles should pass. This method of detection allows what ACTs could not provide: very high duty cycles (close to 100%) and very wide field of view ($\sim$2 sr). These advantages make particle shower arrays a suitable method to observe transient events such as GRBs, despite the fact that the point-source sensitivity of these detectors is almost two orders of magnitude worse than the best ACTs (Hinton & Hofmann, 2009). As mentioned in the previous section, a marginal detection of TeV γ-rays from GRB 970417A was reported by *Milagrito* which is a particle air-shower detector array.

The main challenges faced by particle air-shower detectors is the discrimination of γ-ray showers with hadronic showers. One way to solve this problem is to put the detector at a high altitude in order to achieve a lower energy threshold (less than 1 TeV). Another way is to put the detector deep undegroud and observe high-energy muons which constitute the penetrating component of the shower. Muons from electromagnetic showers could be produced from hadronic photoproduction and the subsequent pion decay, as well-as direct pair-production of muons from the interactions of γ-rays with atmospheric nuclei (Stanev, Vankov & Halzen, 1985; Halzen, Kappes & Ó Murchadha, 2009). Although the number of muons produced in an electromagnetic shower is relatively small compared to hadronic showers, a targeted search to a known source could produce a statistically significant excess over background.

In the 1980s there were a number of repeated detections of γ-ray-induced muons. Samorski & Stamm (1983) from the Kiel experiment and Marshak et al. (1985) from the Soudan-1 detector have detected muons from γ-rays with energies of 10^{15} to 10^{16} eV originating from the binary X-ray source Cygnus X-3, while Dzikowski et al. (1983) from the Łodz group detected a muon excess from γ-rays with energies of at least 10^{16} eV from the Crab Nebula. Despite a promising start, interest in this method however appears to waned in the following decades (Weekes, 2003).

The high-altitude water Čerenkov approach pioneered by *Milagro* proved to be more successful, with contributions to the catalog of TeV sources (Abdo et al., 2007) and surveys of the diffuse γ-ray

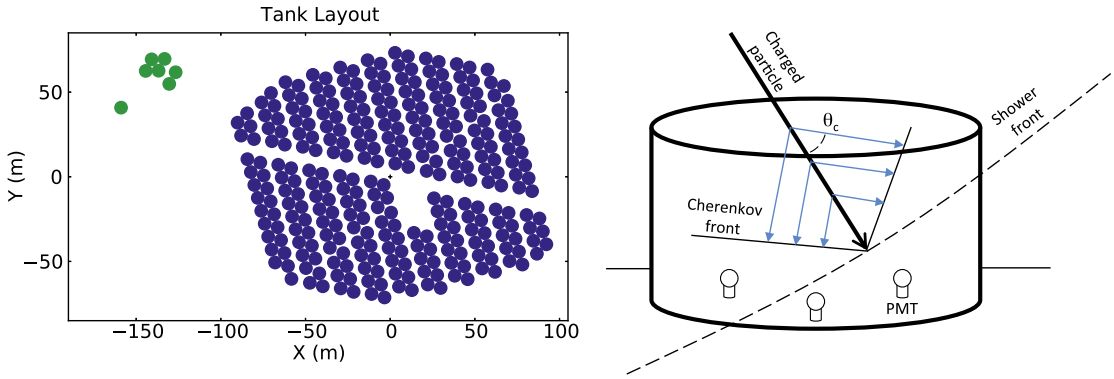

Figure 1.19: HAWC layout and operation principle. *Left:* The relative position of HAWC tanks (blue). The seven tanks at the top left are initial test array. *Right:* The principle of water Čerenkov detection. Particles produced in an air shower arrive at the ground and produce Čerenkov photons as they travel in the water tanks. The photons are emitted at a characteristic angle θ_c with respect to the particle track. The photons will be detected by the photomultiplier tubes at the bottom of the tank. Figures reproduced from (Abeysekara et al., 2012).

[24] http://hawc.umd.edu/

emission of the Milky Way (Abdo et al., 2008). As we have seen in the previous section, Tibet ASγ has also demonstrated the ability to detect TeV γ-rays from the Crab Nebula and several AGNs.

The High-Altitude Water Čerenkov (HAWC) observatory[24] will be the successor of *Milagro* and is expected to be completed in 2014. Located near the peak of Volcán Sierra Negra, Mexico, at an altitude of 4100 m, HAWC will consist of 300 steel tanks of 7.3 m diameter and 4.5 m deep, covering an instrumented area of about 22 000 m^2 (Figure 1.19). Each tank is filled with purified water and will contain four photomultiplier tubes (PMTs): three 20 cm PMTs will be placed near the bottom of each tank looking up to efficiently measure Čerenkov light, and an additional 25 cm PMT with higher quantum efficiency will be placed at the center of each tank. With sensitivity 15 times higher than *Milagro*, HAWC is expected to observe the brightest GRBs with significance of at least 5σ (Abeysekara et al., 2012).

1.4 *The rise of neutrino telescopes*

Ideas to search for cosmic neutrino sources other than the Sun emerged soon after the discovery of Cowan et al. (1956) was published. In 1960, Kenneth Greisen (Figure 1.20) proposed to build a 3000 tons underground neutrino detector to observe the Crab Nebula. Although he admitted that the rate of cosmic neutrino events will be low, Greisen nevertheless was optimistic that "neu-

trino detection will become one of the tools of both physics and astronomy" (Greisen, 1960). On a more pessimistic note, Frederick Reines noted that "the problem of detecting the cosmic ray neutrino appears to be a most formidable one," and warns that "the probability of a negative result even with detectors of thousands or possibly hundreds of thousands of gallons of CCl_4 tends to dissuade experimentalists from making the attempt" (Reines, 1960). In other words, one must possess extreme patience and a readiness to face disappointment to undertake such an effort. Later on Soviet physicist Moisey Markov proposed "to install detectors deep in a lake or in the sea to determine the direction of charged particles with the help of Čerenkov radiation" (Markov, 1960). To isolate the neutrinos from cosmic-ray backgrounds it is necessary to observe neutrinos that have passed through the Earth since "all known particles with the exception of neutrinos are absorbed by scores of kilometres of the substance and thus are entirely screened by the planet" (Markov, 1961).

Figure 1.20: Kenneth Greisen in 1971, here shown celebrating a balloon flight which was the first to detect pulsed γ-rays with energies greater than 200 MeV from the pulsar in the Crab Nebula. Credit: David Koch, Cornell University.

Even neutrinos with extremely-high energy can pass through a detector and remain undetected. The few that interact could create muons as well as electromagnetic and hadronic secondary particle showers. These charged particles will then produce Čerenkov photons that can be detected by a three-dimensional array of photomultiplier tubes that comprise the detector. In the years following Markov's proposal, it was realized that the detector must be of at least a cubic kilometer in size.

In view of these requirements, three open and transparent media came into mind: the atmosphere, water, and ice. Instrumenting the atmosphere with omnidirectional detector does not provide sufficient shielding against cosmic-ray backgrounds. Furthermore, it is constantly lit-up by the Sun and the Moon except for only $\sim$10% of the time (Roberts, 1992).

Water is another option that give several advantages: If the detector is deep enough ($\sim$2–4 km from the surface), sunlight can not penetrate the depth and the layer above it could provide sufficient shielding against the muon background from cosmic rays. Water also has excellent optical qualities, with relatively long absorbtion and scattering lengths that lead to a good angular resolution in reconstructing the direction of the muon.

Water is however contaminated with light from two sources: intermittent light from bioluminescent marine life present at all depths and radioactive decays of ^{40}K that yields a constant rate of optical noise. There are numerous technological challenges in installing an array of detectors at the bottom of the sea. The photomultipliers must be encased in a transparent yet protective shell able to withstand the very high pressure of sea water (roughly 100 atmospheres per kilometer of depth) and the corrosive salt water. In addition, there must be a method to constantly monitor the positions of the photomultipliers which are changing due to the sea currents.

Ice provides a stable platform to work with and the optical background in the sterile ice is low. The scattering length of ice is however shorter than water leading to a lowering of the angular resolution.

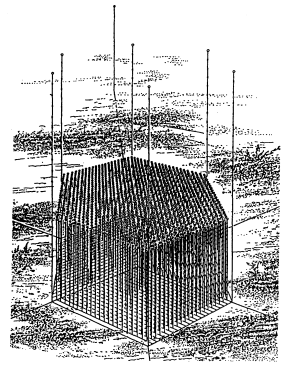

Figure 1.21: The early design of DUMAND: More than 20 000 photomultipliers are arranged in a hexagonal array 800 m on a side. The photomultipliers are tied into strings, each strings consist of 18 photomultipliers. There are 1261 strings, each spaced 50 m apart from each others. Figure reproduced from Roberts (1992).

THE FIRST and heroic effort to construct a large-scale neutrino detector was by the DUMAND[25] Collaboration. An early history of DUMAND was excellently written by Roberts (1992) and will be summarised here. The genesis of DUMAND happened in the 1973 International Cosmic Ray Conference in Denver, when a small group of physicists conceived an undersea muon detector to clarify an anomaly observed in the cosmic-ray depth-intensity curves. The anomaly disappeared later-on when other experiments were made, but it was realized that such an undersea muon detector could also be a neutrino detector. Most of the members of the group then agreed to put the idea of building an undersea muon detector into reality. Thus DUMAND was born.

During a series of DUMAND workshops between 1975–80, it was decided to deploy the detector 30 km off the coast of the Island of Hawaii, at a depth of 4.8 km. The ambitious early design was to construct a detector with 1.22 km^3 volume, consisting of 20 000 photomultiplier tubes arranged in 1261 strings (Figure 1.21). Budgetary and technological constraints forced a constant redesign that considerably reduced the size of the detector after each iteration. The first of such was in 1980 which reduced the number of photomultipliers into 6000 and the volume into 0.6 km^3. Another redesign in 1982 reduced again the size of the de-

[25] Deep Underwater Muon And Neutrino Detector, `http://www.phys.hawaii.edu/dmnd/`

It is interesting to note that Frederick Reines is in fact one of the physicists who conceived DUMAND and he was even the one who named it so (Roberts, 1992).

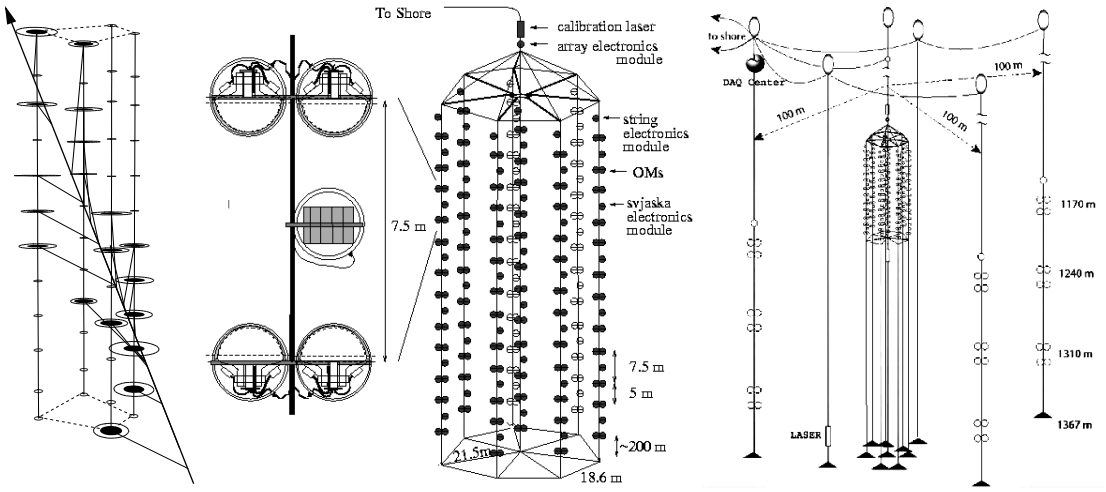

Figure 1.22: *Left:* One of the first upgoing muons from a neutrino, observed using the 4 strings of the detector in 1996. Figure reproduced from Balkanov et al. (1997). *Middle:* The design of the NT200 array of the Baikal Neutrino Telescope. Credit: Baikal Neutrino Telescope, `http://baikalweb.jinr.ru/`. *Right:* The upgraded Baikal Telescope NT200+: the old NT200 surrounded by three external long strings at 100 m radius from the center.

tector into 756 photomultipliers and a volume of 0.03 km^3, which also met the same fate with previous designs. The design that was finally accepted was a 9 strings detector, each with 24 photomultipliers, for a total of 216 photomultipliers. The strings were arranged in octagonal configuration, 40 m on a side, with the ninth string placed at the center.

In December 1993 the first string was finally deployed (Grieder, 1995). The deployment was a success. Unfortunately a leak occured in one of the electrical connectors, resulting in a short circuit and a complete breakdown after 10 hours of operation. Despite a successful recovery of the damaged string one month later, in mid 1996 the US Department of Energy terminated further support and thus the venture to establish the first undersea neutrino telescope met its tragic end.

Lake Baikal in Siberia, Russia, is the deepest fresh water lake in the world and it is here that the venerable Baikal Neutrino Telescope[26] is located. Several of the Soviet scientists involved in Baikal were previously part of the DUMAND Collaboration, however in the early 1980s they were excluded from the Collaboration because the Reagan administration threatened to cut funding should Soviet collaborators be involved (Roberts, 1992).

[26] `http://baikalweb.jinr.ru/`

The Baikal telescope is located in the southern part of Lake Baikal, 3.6 km from the shore at a depth of 1366 m. The first string of photomultipliers was deployed in 1984 and the first muons were detected soon afterwards (Bezrukov et al., 1984). In 1993 Baikal became the first collaboration to deploy three strings of photomultipliers (three is the minimum number of strings required for full spatial reconstruction of muon tracks) and was also the first to report the detection of a neutrino underwater (Figure 1.22, left). In April 1998, 192 photomultipliers were deployed in an array designated as NT200. The photomultipliers are supported by eight strings attached to an umbrella-like frame on top of them (Figure 1.22, middle). The configuration spans 72 m in height and 43 m in diameter.

Baikal is still taking data and upgrades are still carried out. Between February and April the lake is covered with a thick layer of ice, providing a convenient working platform for the construction and maintenance works. In 2005–07 Baikal was fenced by three distant, longer outer strings containing 36 photomultipliers in total (Figure 1.22, right). With this additional strings, named NT200+, the sensitivity of Baikal was increased by a factor of 4 (Aynutdinov et al., 2006).

The Baikal Collaboration will assure the continuing presence of a neutrino telescope in Lake Baikal with the plan to install the Gigaton Volume Detector (GVD). GVD will consists of strings grouped in clusters of eight (Figure 1.23). Each string will carry 24 photomultipliers spaced uniformly from a depth of 900 m down to about 1250 m depth. It is expected to achieve a detection volume of 0.3–0.8 km^3 for muons above 50 TeV (Avrorin et al., 2011).

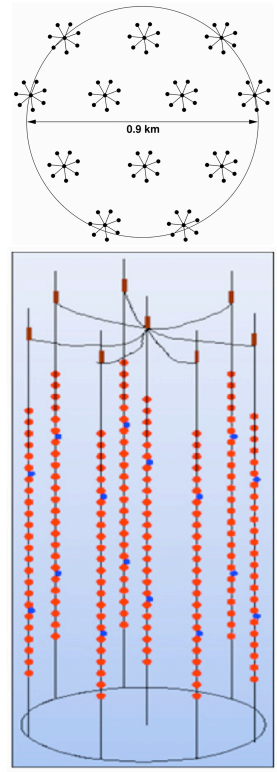

Figure 1.23: The design of the Gigaton Volume Detector (GVD). *Top:* Top view of GVD, showing the arrangement of the 12 clusters. *Bottom:* Schematic view of a cluster, containing 8 strings with 24 photomultipliers in each string. Figure reproduced from Avrorin et al. (2011).

Efforts to establish a neutrino observatory in ice was pioneered by the AMANDA Collaboration[27] in the late 1990s (Andrés et al., 2001). It was built in the 3 km-thick ice sheet at the Amundsen-Scott South Pole Station. Strings with photomultipliers are deployed into the ice by first drilling holes of 60 cm diameter into the ice with pressurised hot water. The strings are then lowered into the hole which subsequently refreezes.

During the 1993–94 Austral summer, 80 photomultipliers encased in protective vessels and mounted on four strings were low-

[27] Antarctic Muon and Neutrino Detection Array, `http://amanda.uci.edu/`

ered into depths between 800 and 1000 m. No muon tracks were however observed. The problem was due to air bubbles trapped in the ice that makes the scattering length became as short as 50 cm, making track reconstruction impossible (Askebjer et al., 1995).

By observing that the scattering tends to decrease with depth it was predicted that the bubbles should disappear at a depth below 1400 m, as the high pressure would cause the bubbles to collapse. The deployment of four additional strings at depths between 1500 and 2000 m during the 1995–96 summer proved this to be the case, as analyses of the data showed that the scattering length is $\sim$20 m. While this is still considerably worse than water, nevertheless it is sufficient for track reconstruction (Ahrens et al., 2004). By 2000, AMANDA was completed, with 19 strings and 677 photomultipliers.

IceCube, the successor of AMANDA, began construction in January 2005. It consists of 5160 photomultipliers mounted on 86 strings at depths of 1450–2450 m (Figure 1.24). The 86 strings are spaced 125 m from each other, covering a surface area of roughly 1 km^2. The photomultipliers are attached to the strings and vertically spaced 17 m from each others. An additional six strings, called DeepCore, are situated in the inner part of IceCube, spaced 72 m apart from each others. DeepCore strings have 50 photomultipliers per string and is installed in the very clear ice at depths between 2100 and 2450 m, where the efective scattering length is at least 50 m. The photomultiplers used in DeepCore strings have an enhanced quantum efficiency. This tighter spacing, better ice quality, and higher effiency of the photomultipliers give DeepCore a lower energy threshold, possibly as low as 10 GeV (Halzen & Klein, 2010). IceCube was completed in 18 December 2010, when its 86th string was deployed. It is currently the largest neutrino telescope in the world.

DUMAND's efforts to establish an undersea neutrino telescope is continued by European groups. The NESTOR[28], ANTARES, and NEMO[29] collaborations were established to explore the possibility of constructing an undersea neutrino telescope in the Mediterranean Sea. After an extensive research and development campaigns, the general atmosphere was an optimistic feeling that the

[28] Neutrino Extended Submarine Telescope with Oceanographic Research, http://www.nestor.org.gr

[29] Neutrino Mediterranean Observatory, http://nemoweb.lns.infn.it/

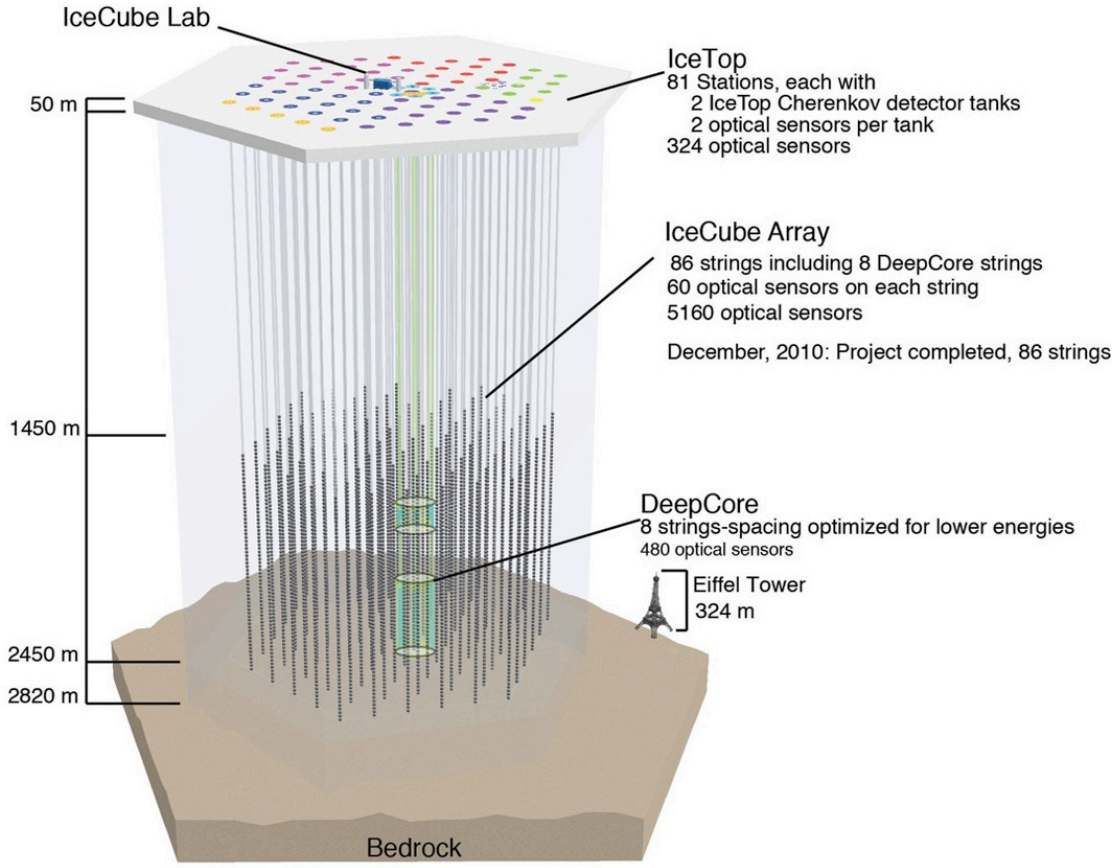

Figure 1.24: Schematic view of the IceCube Neutrino Observatory, with 5160 photomultiplers in 86 strings within 1 km^3 of natural ice. Also shown is the location of AMANDA and DeepCore. The Eiffel Tower is also shown as a size comparison. Credit: IceCube, `http://icecube.wisc.edu/`.

technological challenges to built an undersea detector has been overcome (ANTARES collaboration, 1997).

The ANTARES neutrino telescope was completed in 2008, proving that such an instrument is now within technological reach. It is currently the largest underwater neutrino telescope in the world and data are routinely taken. The detector is located at a depth of 2475 m, 40 km off Toulon, south of France. It consists of 12 detector strings, 11 strings have 25 floors with 3 photomultipliers and 1 string has 20 floors with 3 photomultipliers. The strings are anchored to the seabed and kept upright by a buoy at the top. Because of the long scattering length of more than 250 m and accurate positioning of all photomultipliers, muon tracks can be re-

constructed with precision of $\sim 0.2^\circ$ for muons of energies greater than 1 TeV (Brunner, 2011). More technical details on the ANTARES neutrino telescope and its track reconstruction technique will be described in Chapter 6.

The ambition to build a km-scale undersea neutrino telescope is continued by the KM3NeT Collaboration[30], which was formed by the previously mentioned European groups together with deep-sea technology and marine science groups. The technical design phase has been completed. The first string of KM3NeT is expected to be deployed in 2013 and construction is expected to be completed in 2020.

[30] km^3 NEutrino Telescope, http://www.km3net.org/

1.5 *This thesis: Neutrino telescopes as γ-ray observatories*

NEUTRINO telescopes can also operate as γ-ray observatories by observing the muon component of photon showers. With the establishment of very large volume neutrino telescopes in the last five years and plans to build larger telescopes, it is timely to revisit this old idea and analyse the now-available data.

The muon component of electromagnetic showers is however produced in small numbers. Thus the sensitivity of neutrino telescopes to γ-rays is weak. Muons induced from cosmic rays interacting with the atmosphere will be the main background. The thick layer of water or ice above the neutrino telescope provide shielding that reduces the background—as we shall see later on from analysis of ANTARES data in Chapter 8—to a small amount.

In principle this method of detection is applicable to any known TeV γ-ray sources, for example supernova remnants in the Galaxy or nearby AGNs. In reality, however, their measured fluxes are in the order of $\sim 10^{-11}$ TeV^{-1} cm^{-2} s^{-1}, which is much too low to be detected by neutrino telescopes (Halzen, Kappes & Ó Murchadha, 2009). After all, these TeV sources are steady sources and can be studied better with atmospheric Čerenkov telescopes.

GRBs are however an attractive target for neutrino telescopes due to the large flux of γ-rays during a very short time. Despite the fact that most of GRBs are located at cosmological distances, on rare occasions nearby GRB events do occur. The high duty cycle and wide field of view of neutrino telescopes are suitable to

observe nearby GRBs. Should a nearby GRB occur within the field of view of a neutrino telescope, detecting TeV γ-rays allows us to put constraints on the mechanisms of GRB jets and to search for origin of cosmic rays. Moreover, background can be considerably reduced by localizing the search to the specific direction and time of where and when the GRB happened.

Another way that can possibly increase the sensitivity of neutrino telescopes is by looking at the raw data when the GRB happened. Due to the large amount of data, filtering algorithms are employed to record events that are possibly caused by the passage of muons in the detector. However, the analysis of the raw data that coincide with a known GRB event can possibly lower the detection threshold and thus increase the potential to discover γ-ray signals from GRBs. The trigger to save all raw data can be provided by spaceborne γ-ray observatories that routinely detect $\sim$1 GRB per day. Together they form the GRB Coordinates Network (GCN)[31], a system that distribute alert notices to its subscribers whenever any spacecraft that is part of this network detects a potential GRB (Barthelmy et al., 2000). Neutrino telescopes can use these alert information to save all raw data for offline analysis. At present five satellites are part of this network: HETE (Ricker et al., 2003), INTEGRAL[32] (Winkler et al., 2003), *Swift*[33] (Gehrels et al., 2004), *Fermi* (Moiseev, 2008), and AGILE[34] (Cocco et al., 2002).

[31] http://gcn.gsfc.nasa.gov/

[32] INTErnational Gamma-Ray Astrophysics Laboratory, http://www.esa.int/esaMI/Integral/

[33] http://heasarc.nasa.gov/docs/swift/swiftsc.html

[34] Astrorivelatore Gamma a Immagini LEggero (Light-Imaging Gamma Astrophysical Detector), http://agile.rm.iasf.cnr.it/

Despite these potentials, detecting the TeV component of GRBs is not without pitfalls. One of the main problems that comes to mind is the attenuation of TeV γ-rays by ambient IR photons in the universe. Along their path from the source to the Earth, TeV γ-rays collide with ambient IR photons and annihilate themselves, creating pairs of electron–positron in the process. The cross section for such process is well-known but measuring the accurate spectral density of cosmic IR photons at all redshifts is still a main problem. This problem will be discussed in more details in Chapter 2 by confronting current attenuation models with observational data. This attenuation will limit possible observations only to the nearest GRBs.

Another crucial problem is to calculate the number of detectable muons produced from a γ-shower. Two production mechanisms

are identified: photoproduction and direct muon-pair production. Both mechanisms have a small cross-section process and different energy dependence. The two mechanisms will be discussed in more detail in Chapter 3 and the necessary formula to determine the number of muon produced from γ-showers will be provided. In calculating the observed muon flux at detector level, the muon energy loss caused by their passage through seawater (Section 3.6) should also be taken into account. Using all this, the number of detectable muons for single GRB events at different redshifts are calculated (Chapter 4), as well as the prospect of detecting signal events from stacked GRB data (Chapter 5).

It is also necessary to quantify the performance of the detector. Part II of this dissertation will cover this question. After a description of the ANTARES neutrino telescope and the reconstruction technique in Chapter 6, simulations of the response of the ANTARES detector to downgoing muons will be described in Chapter 7. The statistical methods employed to analyse the data are presented in Chapter 8 and Chapter 9.

Part III of this dissertation deals with the analysis of the ANTARES data to search for TeV γ-ray signals from potential GRBs. A selection of potential targets among the known GRB events will be presented in Chapter 10, followed by the description of the data analysis in Chapter 11.

The conclusion that can be derived from this first attempt to operate a neutrino telescope as a γ-ray observatory will be discussed in Chapter 12. The overall prospect of this whole venture will also be discussed.